

MICHIGAN STATE UNIVERSITY LIBRARIES

LIBRARY Michigan State University

This is to certify that the thesis entitled

"TWO DIMENSIONAL BUOYANT JET SPREADING LAYERE"

presented by

Bernard Benjamin Sheff

has been accepted towards fulfillment
of the requirements for
Master Civil
of Science degree in Engineering

Date <u>5/24/90</u>

MSU is an Affirmative Action/Equal Opportunity Institution

O-7639

PLACE IN RETURN BOX to remove this checkout from your record. TO AVOID FINES return on or before date due.

DATE DUE	DATE DUE	DATE DUE

MSU Is An Affirmative Action/Equal Opportunity Institution

TWO DIMENSIONAL BUOYANT JET SPREADING LAYERS

Ву

Bernard Benjamin Sheff

A THESIS

Submitted to
Michigan State University
in partial fulfillment of the requirements
for the degree of

MASTER OF SCIENCE

Department of Civil and Environmental Engineering

1989

ABSTRACT

TWO DIMENSIONAL BUDYANT JET SPREADING LAYERS

By

Bernard Benjamin Sheff

The spreading layer of a two dimensional buoyant jet discharged into a two layer ambient field has been studied. The gross characteristics of the spreading layer produced by a buoyant jet when the parameters of the ambient field and buoyant jet are varied, were measured. The parameters of the spreading layer which were of interest included: spreading layer thickness, maximum height of rise, minimum dilution and spreading layer height.

Utilizing dimensional analysis, simple equations were developed which describe the gross characteristics of the spreading layer. The experimental data is utilized to develop the constants for the equations which are presented as a function of the dimensionless strength of the density discontinuities. The experimentally derived equations are compared to estimates made utilizing a numerical model which integrates the integral equations.

In general, the experimentally derived equations can be utilized with less than 10 percent error. However, a narrow transition region was encountered where the equations do not accurately predict observed behavior.

Copyright by
BERNARD BENJAMIN SHEFF
1989

DEDICATION

To my son, Benjamin, and his namesake, Benjamin Cherry Sheff.

ACKNOWLEDGMENTS

As this manuscript will probably be the only work I will ever have placed in a library, this forward must include a considerable number of individuals. First and foremost, I wish to thank my major professor, Assistant Professor Roger B. Wallace. The encouragement he exhibited and his unique way of only showing the direction and allowing me to determine the result were greatly appreciated.

Furthermore, I am indebted to my thesis committee, Professor Reinier J. Bouwmeester, Professor David C. Wiggert and Professor Mackenzie L. Davis. In addition to reviewing the thesis, Professor Davis provided day-to-day guidance and counseling to myself and all graduate students and I hope I have adequately thanked him for his time and assistance.

This research was supported by the Institute of Water Research, grant # 14-34-0001-2124. In addition, I wish to thank the Civil and Environmental Engineering Department for the assistantship to complete my master's work.

A major portion of the technical problems regarding the construction of the laboratory were solved by the technical staff in the MSU Engineering Machine Shop; their assistance was appreciated. Furthermore, I would like to thank Mrs. Lois Pierson for her patience in typing and correcting this manuscript.

Finally, I must mention my family. My mother and father gave me the moral and financial support to complete my bachelor's degree and master's work. My wife has supplied the support to complete this endeavor and given me a son to dedicate this manuscript to.

TABLE OF CONTENTS

	LIST OF TABLES	٧
	LIST OF FIGURES	/i
	LIST OF SYMBOLS	j
	ABBREVIATIONS	×
CHAPTER	R	
1	- INTRODUCTION	1
•		٠
2	BUOYANT JET PHYSICS, PREVIOUS RESEARCH AND PROBLEM STATEMENT	A
	Official Company	4
	2.1 General	4
	2.2 Buoyant Jet Physics	4
	2.3 Previous Research	8
	2.2.1 Spreading Layers in Homogenous Fluids	8
	2.2.2 Studies with Linear Stratifications 1	3
	2.2.3 Non-Linear Stratifications	
	2.2.3 molt-lined Still-lined Still-line Stil	5
	2.3 Problem Statement	. 3
3		8
	3.1 General	8
		8
		2
•		۔ د
4	EXPERIMENTAL APPARATUS AND PROCEDURES	24
•		24
		. ¬ 24
		28
	4.4 Stratification System and Density Measurement 3	11
	4.4.1 Stratification System	11
	4.4.2 Density Measurement	14
	4.5 Dilution Measurement System	15
	A & Diffusion Sustain	, 7
	4.6 Diffuser System) / \
	4.7 Procedures	9
5	RESULTS AND DISCUSSION	4
	5.1 General	4
		4
	5.3 Minimum Dilution	6
		9
		9
	5.6 Summary	2
6	CONCLUSIONS AND RECOMMENDATIONS	4
	APPENDIX A	6
	BIBLIOGRAPHY 6	5

LIST OF TABLES

Table	<u>Pa</u>	ge
1	Summary of Experimental Data 4	3
2	Summary of Results	4

LIST OF FIGURES

<u>Figure</u>		Page
1	Concentration Profiles within a Plume	. 5
2	Schematic of Spreading Layer Produced by a Buoyant Jet Discharged into a Stratified Fluid	. 7
3	Vector Diagram of Fluid Parcel in Non-Linearly Stratified Fluid	. 9
4	Schematic of a Buoyant Jet and Associated Spreading Layer	. 10
5	Generalized Spreading Layer in a Non-Stratified Fluid	. 11
6	Generalized Spreading Layer in a Linearly Stratified Fluid	. 14
7	Spreading Layer Produced when the Themocline Stops the. Rise to the Water Surface	. 16
8	Possible Spreading Layer Classes in Non-Linear Stratification	. 21
9	Plan of Experimental Laboratory	. 25
10	Experimental Tank	. 26
11	Jet Discharge System	. 27
12	Suction Sampling System for Collecting Dilution Samples from the Spreading Layer	. 29
13	The Vaccum Chamber of the Suction Sampling System	. 30
14	Schematic Diagram of the Stratification System	. 32
15	Flow Spreaders for Development of Two Layer System	. 33
16	Jet-Diffuser System	. 38
17	Typical Data Collected during Experiments	. 42
18	Dimensionless Height of Rise	. 45
19 .	Dimensionless Minimum Dilution	47
20	Dimensionless Spreading Layer Height	50

Figure		Page
21	Dimensionless Spreading Layer Thickness	51
22	Maximum Spreading Layer Thickness	53
A-1	Schematic Diagram of a Vertical Slot Buoyant Jet	58

LIST OF SYMBOLS

```
width of jet slot; [L]
p<sup>o</sup>
       kinematic buoyancy flux at the jet source; go'Q [L/T<sup>2</sup>]
В
       local kinematic buoyancy flux: [L/T<sup>2</sup>]
b
       constant value
C
       initial concentration of tracer at source; [M/L3]
co
       concentration of jet' [M/L<sup>3</sup>]
С,
       concentration at any point: [M/L<sup>3</sup>]
C
       maximum concentration in plume; [M/L<sup>3</sup>]
Cm
E
       entrainment coefficient
       gravitational acceleration; [L/T<sup>2</sup>]
q
       effective gravity at the density discontinunity;

g' = g(\rho_1 - \rho_2)/\rho_1; [L/T<sup>2</sup>]
q¹
       local value of g' in any horizontal plane; [L/T<sup>2</sup>]
g'm
       effective gravity at the jet source; go' = g(\rho_1 - \rho_1)\rho_1; [L/T<sup>2</sup>]
qo'
       depth of ambient field; [L]
Н
hs
       thickness of spreading layer: [L]
H1
       depth of lower layer of ambient fluid; [L]
       kinematic momentum flux at the jet source; M = Q^2/b; [L^3/T^2]
M
       local kinematic momentum flux: [L<sup>3</sup>/T]
m
       volume flux at the jet source; Q = wjb_0; [L^2/T]
0
       local plume flux; [L^2/T]
Q
R
       local Richardson Number: [L]
       minimum dilution in the spreading layer; [dimensionless]
Sm
T1
       lower fluid layer temperature
T2
       upper fluid layer temperature
       jet fluid temperature
Tj
```

- Vo local kinematic velocity flux [L/T]
- Wj initial jet velocity; [L/T]
- W time averaged vertical velocity of the jet; [L/T]
- z vertical distance measured from origin; [L]
- Zm maximum height of rise; [L]
- Zs height of spreading layer measured from z=0; [L] general dependent variable
- $_{\rm pj}^{\rm pj}$ jet fluid density at the jet origin; [M/L $^{\rm 3}$]
- P₁ ambient fluid density, lower layer; [M/L³]
- P_2 ambient fluid density; upper layer; [M/L³]
- λ spreading ratio
- ε stratification parameter; [1/T]

ABBREVIATIONS

ZFE zone of flow establishment

CHAPTER 1

INTRODUCTION

An effluent which is buoyant with respect to the receiving body and also possesses momentum is termed a buoyant jet. Buoyant jets are used to discharge waste water, waste gases and thermal wastes into ambient receiving bodies. The mixing produced by a buoyant jet as it rises in the receiving body dilutes the effluent thereby reducing effluent concentrations in the buoyant jet that could be undesirable to the receiving body.

The rise of a effluent discharged as a buoyant jet is initially driven by momentum. However, early in the rise of the of the buoyant jet, buoyant forces may add sufficient momentum to the fluid to overshadow the influence of the initial momentum in which case the buoyant influences domminate the behavior of the plume. The buoyancy driven rise of a jet is caused by density differences between the ambient and the jet fluids, the jet fluid being lighter. The source of the density differences can be temperature or concentration differences between the ambient and jet fluids or a combination of these characteristics. The dilution of effulent density differences produced by the rise of the buoyant jet is the result of ambient fluid being drawn into the jet structure through the process of entrainment.

The buoyant effluent will stop rising when it encounters a reversal of buoyant forces of sufficient strength that the vertical velocity is reduced to zero. Specifically, features of the ambient fluid such as a density discontinuity (i.e. a thermocline), or the water surface can

halt the buoyant jet rise. At the elevation where the effulent rise stops, it will spread out horizontally in a thick layer called the spreading layer. The spreading layer prevents entrainment of ambient fluid into the sides of the jet in that part of the rise occupied by the layer therefore reducing effulent dillution. This effect is referred to as blocking.

The purpose of this research is to characterize the spreading layer produced by two dimensional buoyant jets discharged into nonlinear ambient density stratifications, such as those found in lakes or atmospheric temperature inversions. In addition, determination of effluent dilution produced when a blocking layer was present to reduce entrainment was quantified for the nonlinear density stratifications. The scope of this research involved both experimental measurements and numerical modeling of the buoyant jet, inculding: (a) Construction of the necessary equipment for developing the scaled receiving body and the jet diffuser; (b) Development and calibration of density and dilution measurement equipment; (c) Performance of experiments varying both effluent and ambient body characteristics; and (d) Analysis of experimental data and comparison of experimental results with numerical model predictions.

This thesis is divided into six chapters and an appendix. Chapter 2 presents a review of previous research in the field of buoyant jets and a qualitative description of the physics of buoyant jets. The theory used in the interpretation of observed data is presented in Chapter 3. Chapters 4 and 5 contain experimental procedures and results, respectively. Chapter 6 contains the conclusions and recommendations. Appendix A contains the numerical model B-JETL, developed

for this research, and a cursory review of other numerical models which are currently available for buoyant jet design and analysis.

CHAPTER 2

BUOYANT JET PHYSICS, PREVIOUS RESEARCH and PROBLEM STATEMENT

2.1 General

The physics of buoyant jets has been well developed (Fischer, et al., 1979) and therefore no past literature citings regarding buoyant jets will be included in this chapter. However, a detailed qualitative discussion of the physics envolved with buoyant jets will be provided. Once the general physical problem has been discussed, previous research concerning spreading layers of buoyant jets will be presented in this chapter. Specifically, studies with homogenous, linearly stratified, and non-linearly stratified ambient fluids will be discussed. Although past research has added to the understanding of buoyant jet spreading layers, it is inadequate when applied to the two layer stratified situation. Regarding numerical modeling, a cursory discussion of available numerical models is included in Appendix A with the program, B-JETL, written for the present research. Finally, the problem statement for the current investigation is presented.

2.2 Buoyant Jet Physics

When fluid, initially lighter than the surrounding fluid, leaves the jet origin the cross sectional profiles of buoyancy, velocity, and tracer are initially uniform. The zone of flow establishment, ZFE, occupies a distance equal to 5.2 times the width b_0 of the initial slot discharge. At the end of the ZFE, the characteristics of the profiles have changed from uniform to Gaussian (Figure 1). In general, effluent

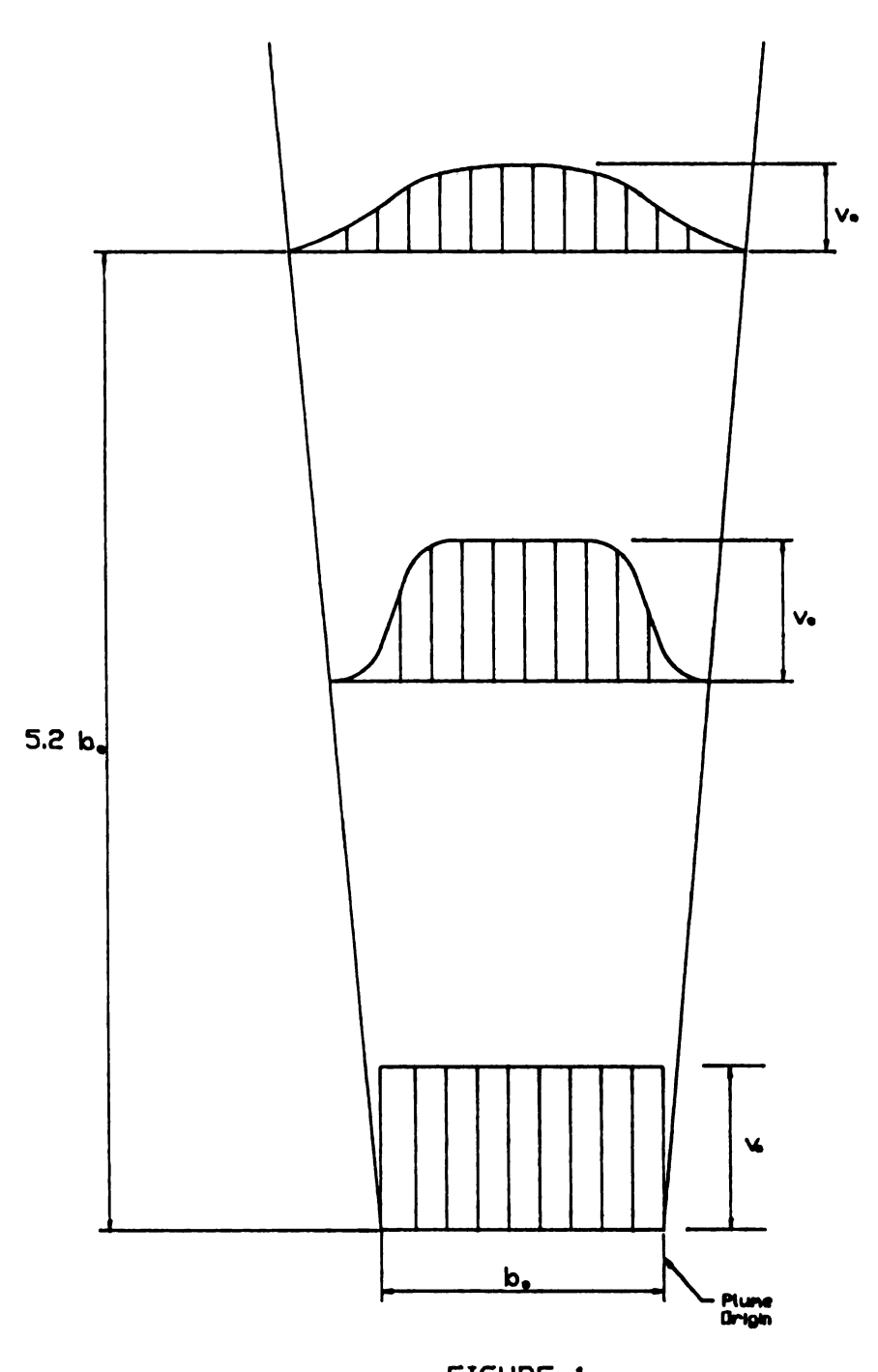


FIGURE 1

Concentration Profiles Within a Plume

is lighter than its surroundings so that both its momentum and buoyancy cause it to rise. The rising fluid causes shear stress between the jet fluid and ambient fluid. In turn, the shear stress produces horizontal movement of ambient flow into the jet. The movement into the jet and subsequent mixing within the jet causes dilution of the tracer in the jet. The entrainment will theoretically continue until fluid ceases to rise. The point at which this occurs is dependent on the ambient fluid. In a homogenous ambient fluid the jet fluid will rise to the surface. In a stratified ambient body, the location where the rise halts is not as easily defined.

In a linear stratified body the jet fluid rises and also entrains ambient fluid (Figure 2). However, with this scenerio the fluid being entrained becomes more like the jet fluid as the rise continues. This occurs because the density of the local ambient fluid varies with depth and it causes the local buoyancy of the jet to decrease. At some point jet fluid will have the same density as the local ambient fluid, i.e. the elevation of neutral buoyancy has been reached. From this point on the jet continues to rise because of its momentum; entrainment continues and buoyancy forces decelerate the rise. When the fluid stops, it is negatively buoyant and tends to fall back toward the point where neutral buoyancy was encountered and spread away from the plume centerline. This spreading away from the plume near the elevation of neutral buoyancy produces a spreading layer.

The previous scenarios have described the case of a buoyant jet in both a non-stratified and a linearly stratified fluid. In a non-linearly stratified fluid, the buoyant jet fluid would initially rise and entrain ambient fluid as described for the homogenous fluid.

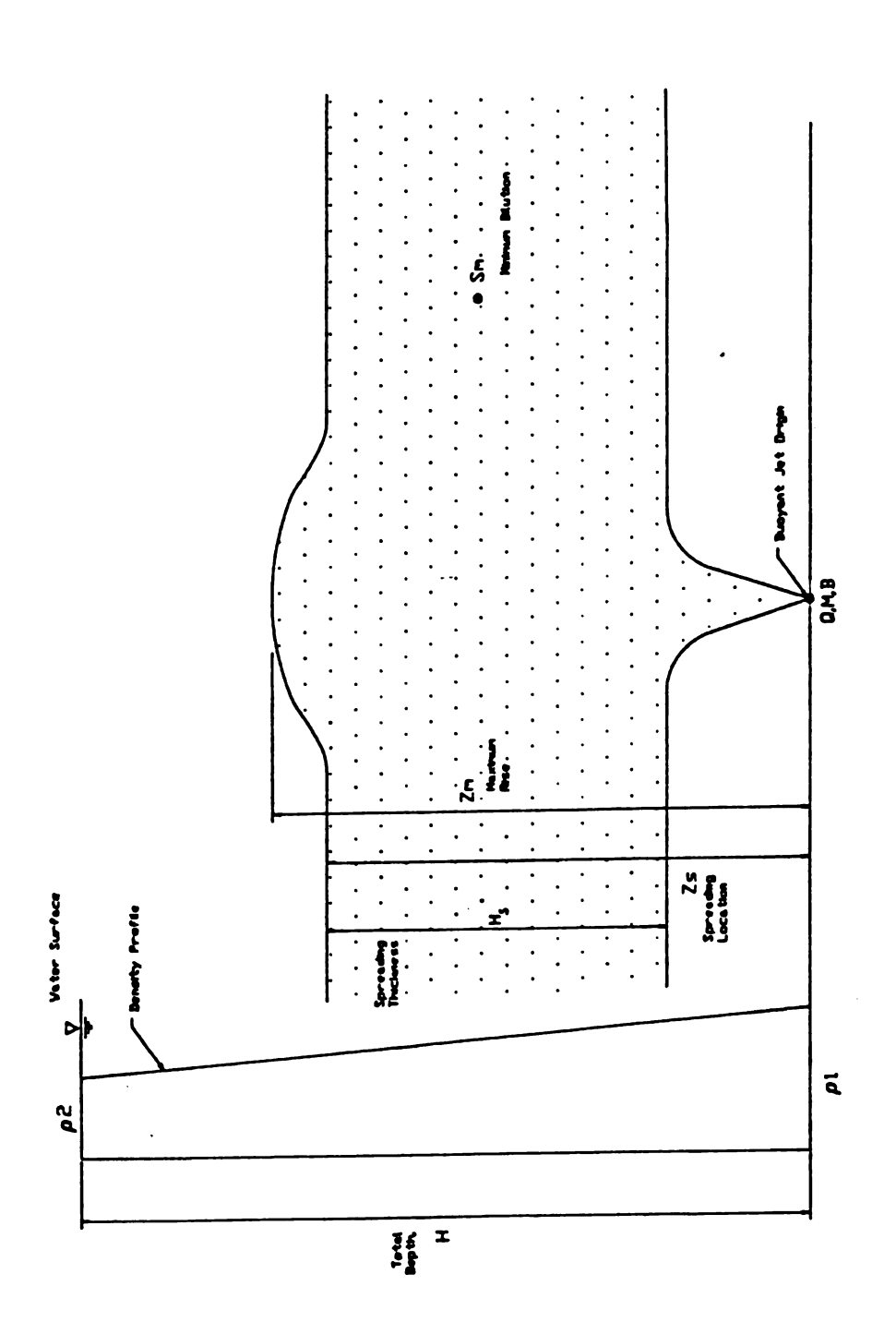


FIGURE 2
Schematic of Spreading Layer Produced by
Buoyant Jet Discharged into a Lineal Stratified Fluid

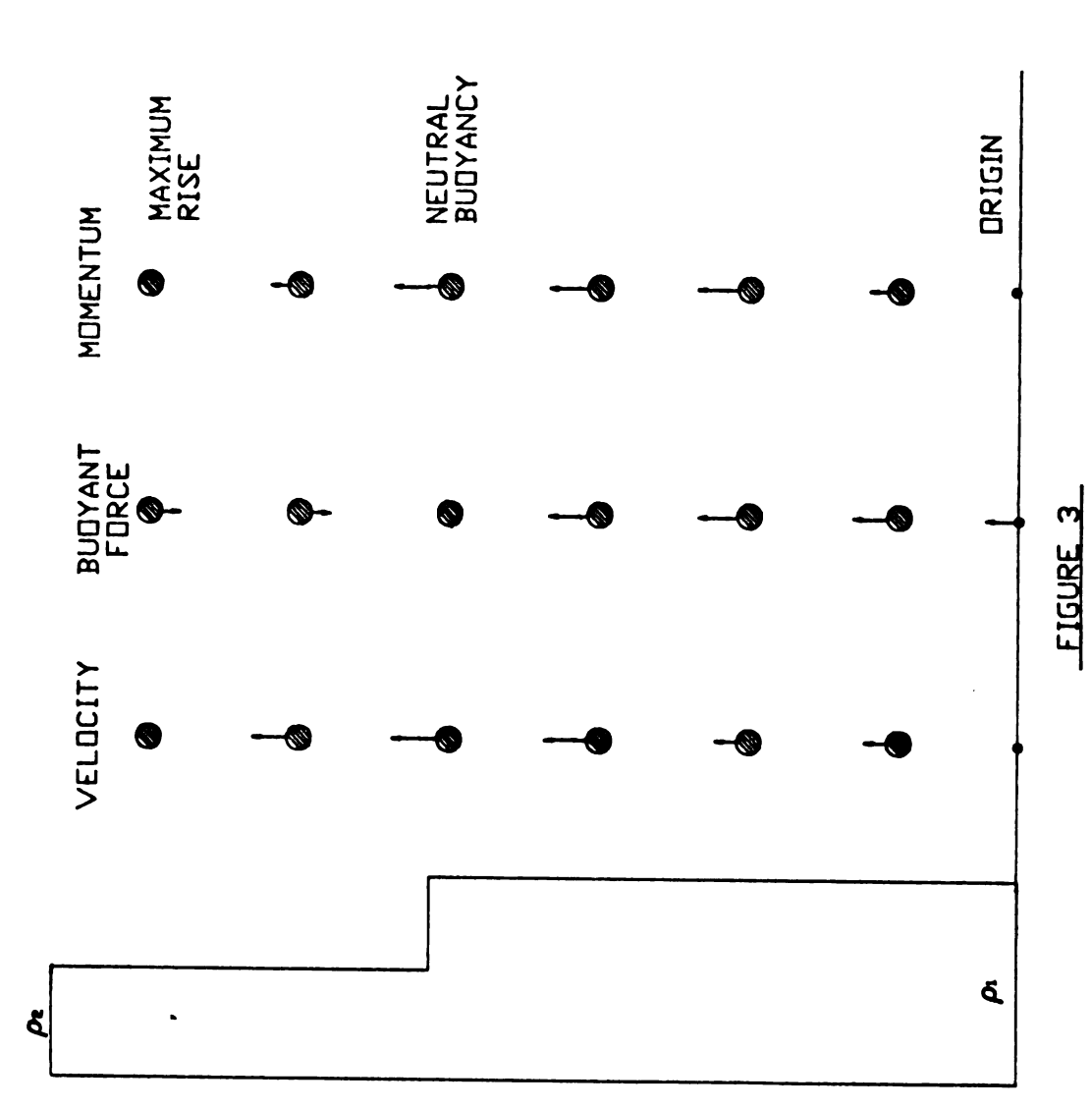
However, once the jet encounters the density disconunity characteristic of the non-linear stratification, jet fluid would behave much like in the linear stratified fluid. If the upper ambient layer has a density close enough to the jet fluid, it can reverse the buoyancy and halt the fluid rise. Conversely, if the upper layer is still heavier than the jet fluid, jet fluid will rise to the water surface. In either case, the spreading layer will form below the location where the vertical motion is halted. A vector diagram which presents the relationship of velocity, buoyancy and momentum for a plume in a non-linearly stratified system is presented in Figure 3. The fluid parcel represents a unit volume of fluid in the plume with the average characteristics (velocity and density) of the plume at that elevation. A schematic of a buoyant jet and the associated spreading layer in a non-linear stratified fluid is shown in Figure 4.

2.3 Previous Research

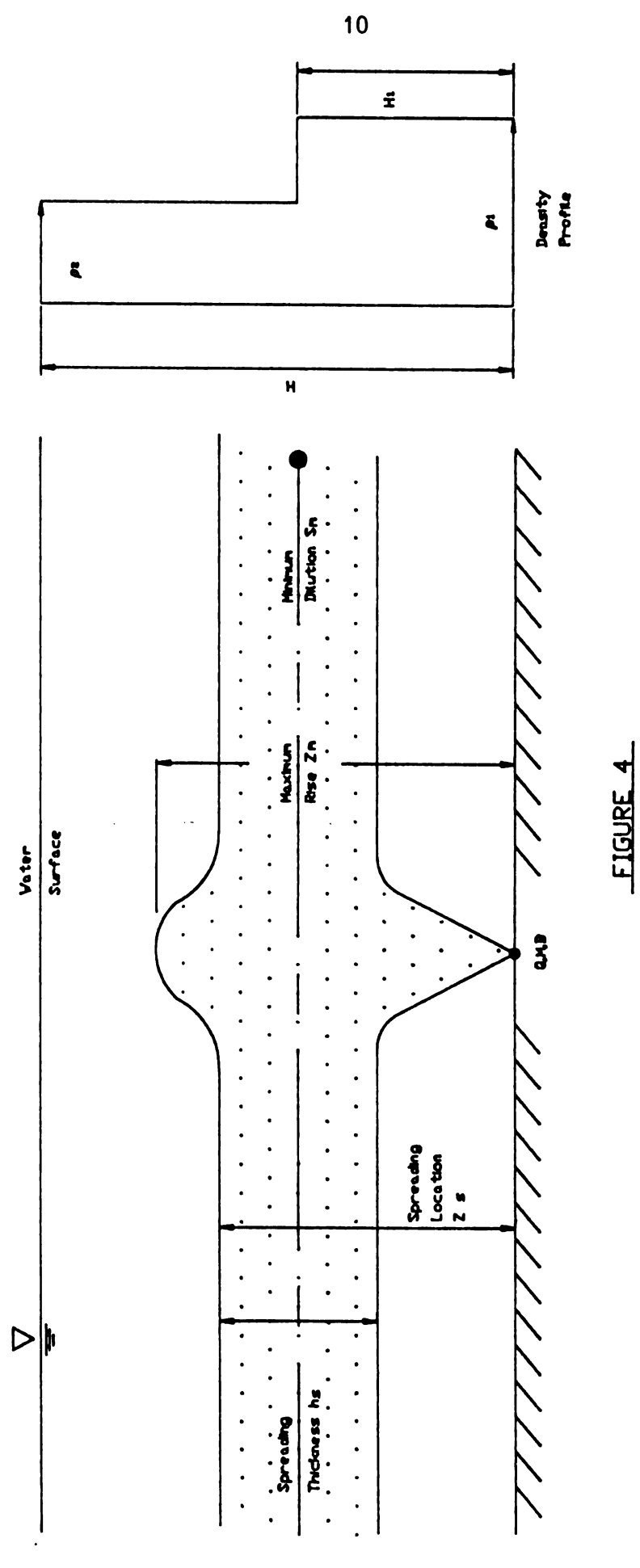
2.3.1 Spreading Layers in Homogenous Fluids

Spreading layers in homogenous ambient fluids were first studied by Jirka and Harleman (1973). Their measurements showed that in a fluid of depth H, a spreading layer thickness of (0.17)H is observed where the fluid first reaches the surface. Furthermore, they predicted the occurance of a hydraulic jump which would cause this initial thickness to increase a short distance from the plume centerline.

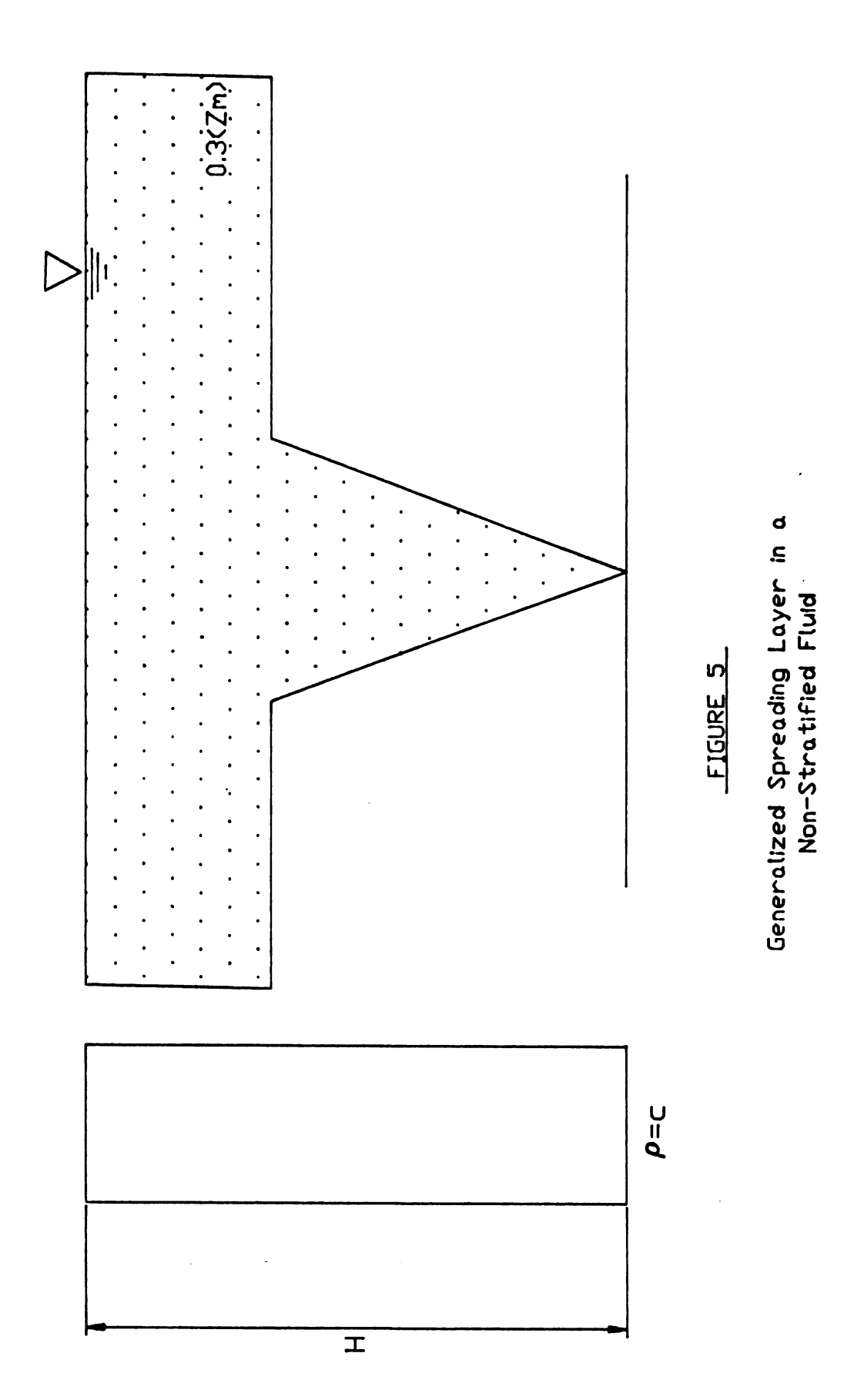
Roberts (1977) presented data which showed a spreading layer thickness of approximately (0.3)H (Figure 5) after the jump described by Jirka and Harleman. In addition, Roberts presented a photograph



Vector Diagram for a Parcel of Fluid Rising Because of Buoyancy in a Non-Linearly Stratified Fluid



Schematic of Spreading Layer Produced by Buoyant Jet Discharged Into two Layered Ambient Fluid



which showed the relative thickness of the spreading layer prior to the jump. Of late, Roberts (1981) offered a procedure to estimate the effect of blocking and locate the spreading layer in a stratified fluid based on his measurment of spreading layer thickness in a homogenous fluid of depth H. Roberts assumed that the spreading layer in a stratified fluid will have a thickness of (.3)Zm, where Zm is the maximum height of rise, and the spreading layer will be immediately below Zm. Furthermmore, he assumed the tracer concentration in the spreading layer was the average concentration because additional dilution which occurs in the area of the spreading layer could only result from mixing (not entrainment) which causes the concentration profiles to be evened out.

Although Robert's studies are adequate for locating the spreading layer and accounting for blocking (the reduction in entrainment due to a spreading layer) in homogenous fluids, they present no clarification of what actually takes place when spreading occurs in stratified fluids.

Koh (1976) studied buoyancy driven gravitational spreading which occurs when a light fluid spreads on top of a heavier, motionless one. He derived equations which showed that after an initial startup time, a two-dimensional continuously discharged fluid spreads with a constant thickness. However, when discharge is allowed to continue for a long time, t, the thickness increased slowly as t¹⁷⁵. This research, although important to determining the thickening of spreading layers in unstratified fluids does not directly predict the effect of blocking on dilutions of the spreading layer.

Finally, a method was offered by Koh (Fisher, et al. 1979) to approximate the influence of blocking on dilutions for both homogenous

and linear stratifications. However, this method was based on sparse experimental results and Koh cautioned that it is only an approximation.

2.3.2 Studies with Linear Stratifications

Buoyant jets discharged vertically into linearly stratified ambient fluids were studied by Wright and Wallace (1980). This research involved the measurement of the gross characteristics of the buoyant jets. Their data showed that buoyant jets in linear stratifications had almost twice the spreading layer thickness as those in homogenous ambient bodies. Furthermore, the spreading layers had a measured thickness of (0.51)Zm where Zm was the maximum height of rise. In addition, the top of the spreading layer was located a distance (0.17)Zm below the maximum rise point (Figure 6). With this extensive blocking being caused by the spreading layer, only (0.32)Zm is available for entrainment. An interesting side note was that the spreading layers produced by pure jets were thicker than those from plumes in the linear stratification.

Furthermore, the minimum dilutions, Sm, measured in the spreading layer agreed well with the integral equations predictions of minimal dilution at Zm. This was achieved using a numerical model with an entrainment coefficient which was linearly dependent on the local Richardson number ($R = \beta q^3/m^3$). In addition, the calculated values of Zm and minimum dilution included no correction for blocking. When a blocking correction was made the dilutions calculated were 40 percent less than those measured. Therefore, using a blocking correction in design applications could produce a diffuser 2.5 times longer than required.

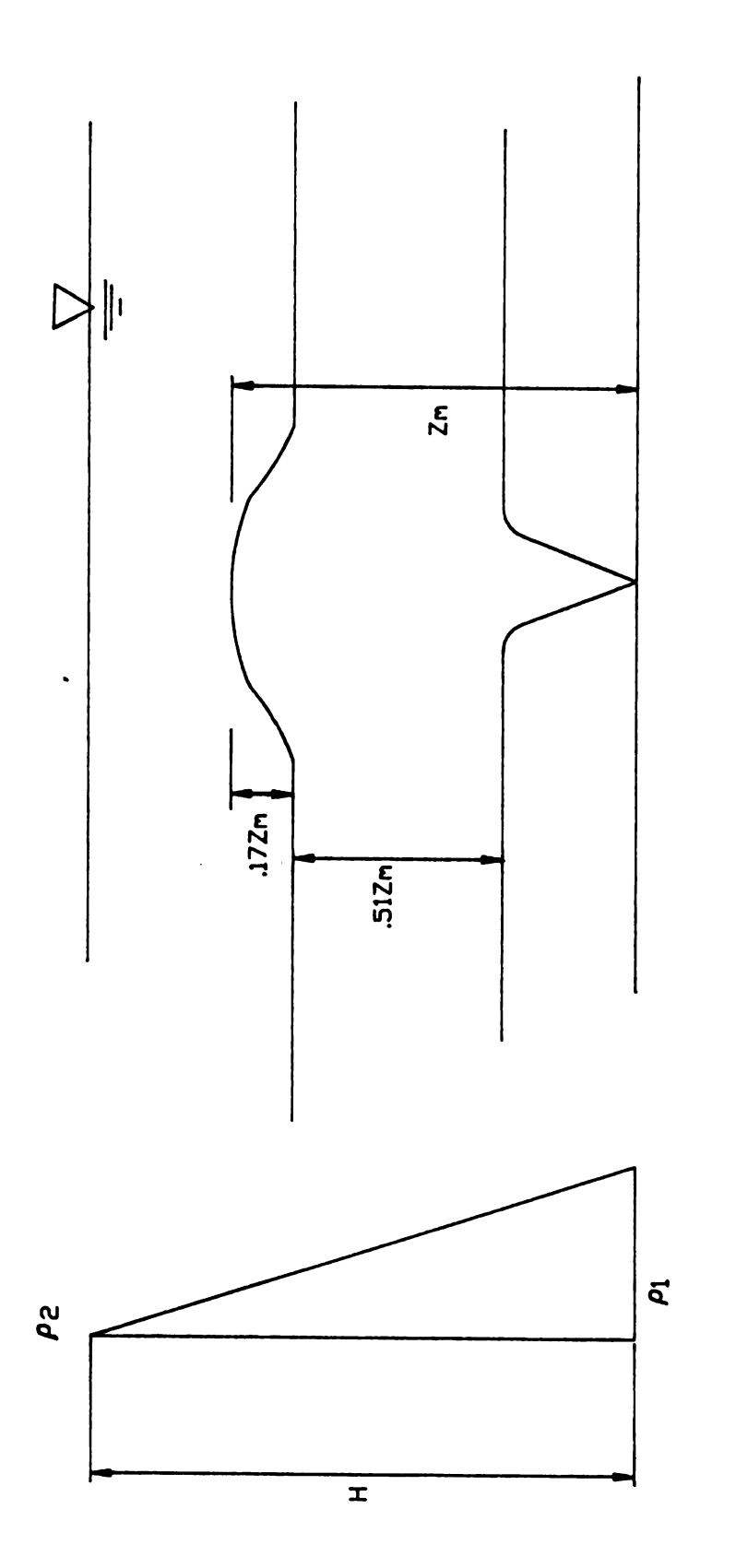


FIGURE 6 Generalized Spreading Layer in a Linearly Stratified Fluid

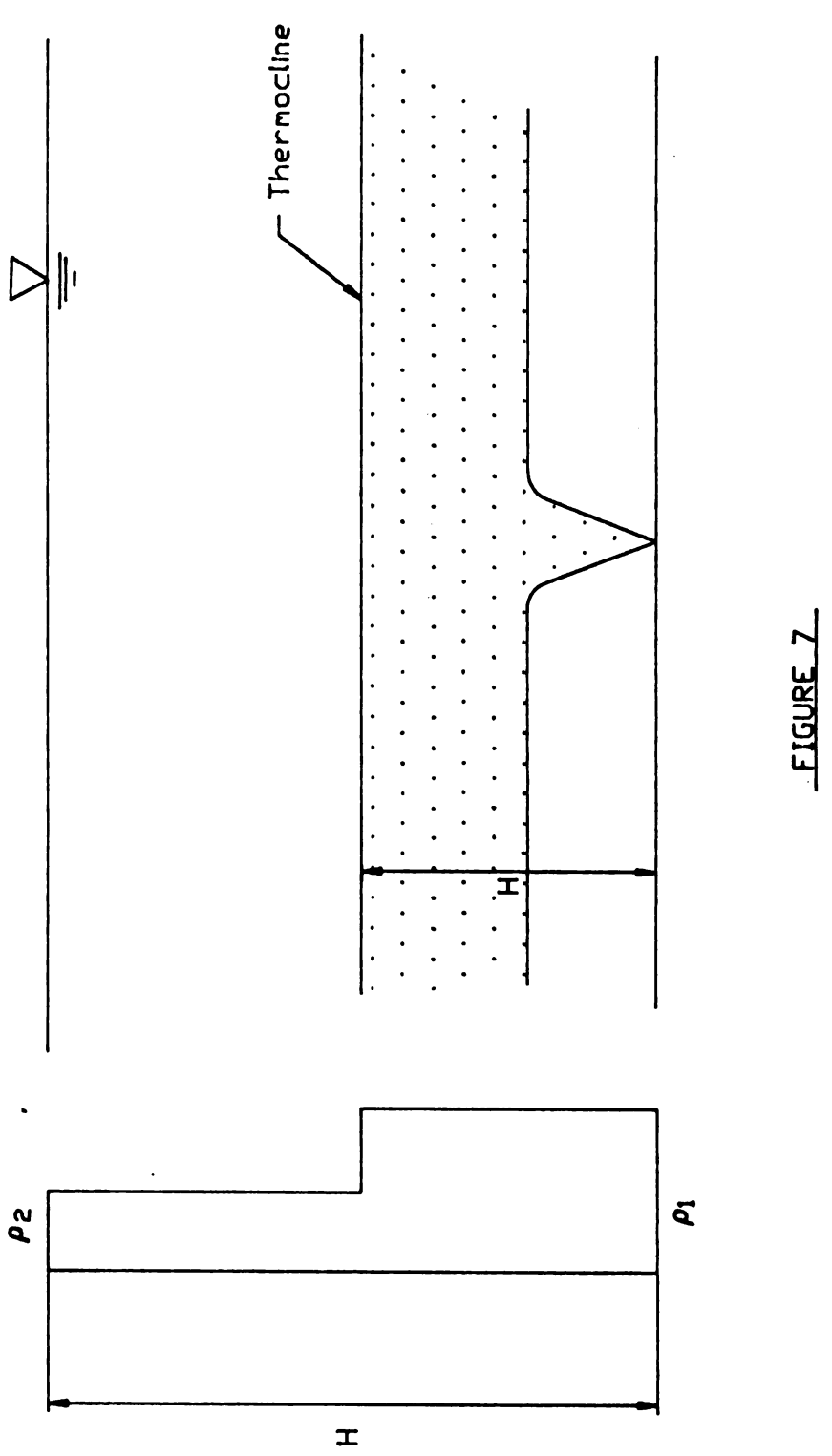
2.3.3 Non-Linear Stratifications

Scant research has been reported in the area of buoyant jets rising in non-linear stratifications. Hart (1961) studied the effects of a thermocline on an axi-symmetric plume. He determined a dimensionless parameter which predicted the elevation of the center of the spreading layer. These equations were scaled by the initial jet diameter. However, Wallace and Wright (1979) showed that the jet diameter may be of minor importance as a scale parameter in which case it should not be used for scaling. In addition, Hart's method did not give satisfactory values to predict spreading layer thickness from initial plume conditions.

Roberts (1981) suggested estimating the blocking effect in non-linear stratifications by applying the same method which he suggested for homogenous fluids (See Section 2.2.1). However, Roberts used the height to the epilimnion, H1, instead of Zm in the calculations. This calculation method could then be used in the case where the thermocline is strong enough to stop the plume from reaching the water surface. There appears to be no data to deter- mine the adequacy of this approach.

2.4 Problem Statement

From the previous discussion of past research it is obvious that prediction of spreading layer characteristics such as location, thickness and dilution are at best an approximation. The purpose of this research is to determine the effects of non-linear stratifications on the maximum rise and minimum dilution of buoyant plumes, and the thickness and height of the spreading layers produced. In addition, a



<u>FIGURE 7</u> Spreading Layer Produced When the Thermocline Stops the Rise to the Water Surface

numerical model will be tested to determine its ability to predict plume characteristics. A large range of non-linear density profiles will be used to determine plume characteristics over a wide range of conditions. Finally, dimensionless equations will be derived which will predict plume and spreading layer characteristics.

CHAPTER 3

THEORY

3.1 General

The purpose of this chapter is to present the theory which was used to analyze the experimental data and in development of the numerical model.

3.2 Theory for Data Analysis

Two-dimensional buoyant jets can be characterized by initial fluxes of kinematic buoyancy B, kinematic momentum M, and volume Q (Wright and Wallace, 1979). The ambient fluid can be characterized by the effective acceleration, $g'=g(\rho_1-\rho_2)/\rho_1$, the bottom layer thickness, H1, and the total depth of fluid, H. Any of the spreading layer characteristics of interest, here represented by the general dependent variable θ , are assumed to be related to these independent variables by the equation

$$\phi = f(Q,M,B,g',H1,H)$$
 Eq. 1

with dimensions of the independent variables given as $(L^2/T, L^3/T^2, L^3/T^3, L/T^2, L, L)$, respectively.

Next, the Buckingham Pi theorem of dimensional analysis is utilized in a manner similar to Wallace and Wight (1980). Selecting H, g', and B as the repeating variables, the spreading layer height Zs, thickness Hs, and minimum dilution, Sm, are related to the independent variables by a dimensionless equation of the form

$$\frac{Zs}{H}$$
, $\frac{Hs}{H}$, $\frac{SmQ}{HB^{1/3}}$, $\frac{Zm}{H}$ = $f\left(\frac{H1g^{1}}{B^{2/3}}, \frac{H1}{H}, \frac{H1}{K/B^{2/3}}\right)$ Eq. 2

To obtain Eq. 2, the Boussinesq assumption was made, i.e. that the density differences between the upper and lower layers, and the plume fluid were small compared to any one of these densities and that these density differences affect only bouyant forces. In addition, the initial volume flux was also neglected, meaning that Eq. 2 applies where \mathbf{O}^2/\mathbf{M} is small relative to H1 (the smallest possible rise). The dimensionless minimum dilution was determined using the assumption that the terminal dilution, Qt, was the dependent variable and the minimum dilution was proportional to Qt/Q. Therefore, Eq. 2 states that the dimensionless dependent variables are fixed by the independent variables: $\mathrm{Hig}^4/\mathrm{B}^2/\mathrm{J}^3$, relating the distance to the interface, the strength of the interface, and the initial buoyancy flux B; H1/H, the ratio of the two layers of fluid and $\mathrm{Hi}/(\mathrm{M/B}^{2/3})$, the ratio of the minimum possible rise distance to the point at which the initial momentum is insignificant compared to the momentum generated by buoyant forces.

Using Eq. 2 and letting the initial momentum flux go to zero, the pure plume case can be studied. If momentum flux goes to zero, the term $H1/(M/B^{2/3}$ goes to infinity and the equation simplifies to:

$$\frac{Zs}{H}$$
, $\frac{Hs}{H}$, $\frac{S_mQ}{H/B^{1/3}}$, $\frac{Zm}{H}$ = $f\left(\frac{H1g'}{B^{2/3}}, \frac{H1}{H}\right)$ Eq. 3

As the plume rises to H1, momentum m is generated. At the interface, the local buoyancy flux changes from its initial value B to a smaller value b as fluid crosses the interface. Considering only the relative value of b at the interface, two classes of spreading can be anticipated.

A strong density discontinuity will cause the bouyancy to reverse (b<0<B) and therefore produce a spreading layer below the interface as in

Figure 8A. With spreading occurring below the interface, the total depth in Eq. 3 is not important and simplifies Eq. 3 to:

$$\frac{7s}{H1}$$
, $\frac{SmQ}{H1}$, $\frac{Zm}{H1}$ = constant Eq. 4

Conversely, a weak density discontinuity will allow the plume to rise and to spread just below the water surface (Figure 8B). In this case, even though the buoyancy is reduced at the interface, the reduction is not enough, (0 < b < B), to stop the rise. Applying these circumstances to Eq. 3 where Zm/H = 1 and H1 is not important compared to H, the following equation is written:

$$\frac{Zs}{H}$$
, $\frac{Hs}{H}$, $\frac{SmQ}{HB^{1/3}}$, $\frac{Zm}{H}$ = constant Eq. 5

This is the asymptotic case of a non-stratified homogenous fluid of finite depth.

In a situation where the density discontinuity is of sufficient strength to cause b to be less than or equal to zero, the momentum m generated in the rise to H1 would be expected to cause the plume to rise above H1, and possibly fill the area between H and H1 (Figure 8C). This would occur with a moderate strength stratification.

The parameter H1g'/B^{2/3} should describe all of the different situations. Therefore, the interface strength could be estimated on the basis of a single critical value of this parameter. In strong stratifications (H1g' >>C), in weak stratifications (H1g' \otimes C), and in moderate

stratifications ($\frac{\text{H1g'}}{\text{B}^{2/3}}$ = C). The term H1/H will determine the midpoint distance, between H1 and H, where the plume will terminate in the moderate stratification.

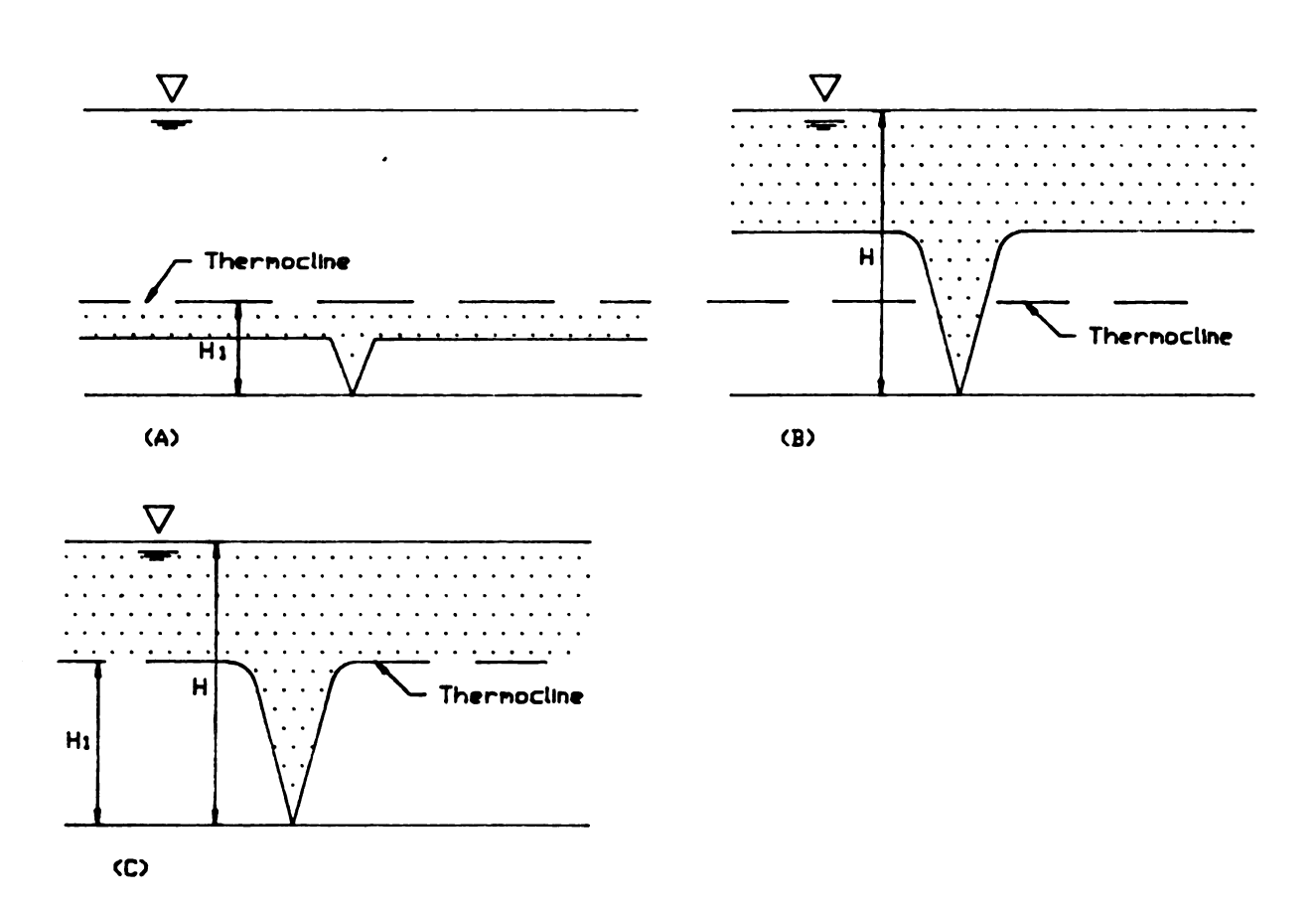


FIGURE 8

Possible Classes of Spreading Layers for a Plume in a Non-Linearly Stratified System: (A) Strong Stratification (B) Weak Stratification (C) Moderate Stratification.

The dimensional analysis above supplies the starting point for characterizing buoyant plume spreading layers. Using the experimental data collected, the appropriate values of C for each dependent variable can be estimated and spreading layer behavior near the buoyant jet centerline can be characterized.

3.3 Numerical Model Theory

The numerical model, although similar to Solti's (1971), was developed specifically for the abrupt density discontinuity employed. This model, which predicted values of Sm and Zm at the jet centerline, solved Eqs. 6 through 8 as initial value problems and carrying the integration through the full height of rise. A Runga Kutta - Verner fifth and sixth order differential equation program was utilized to perform the integration.

$$\frac{dq}{dz} = E$$

$$\frac{dm}{dz} = \frac{bq}{m} \left(\frac{1+\lambda^2}{2}\right)^{1/2}$$

$$\frac{d\beta}{dz} = -q \varepsilon$$

$$\frac{dt}{dz} = 0$$
Eq. 8

Eqs. 6 through 9 above, first derived by Fan and Brooks (1969), are described in detail by Wallace and Wright (1979). The integration started at the zone of flow establishment (z=5.2 Q^2/M) where the Gaussian profile first develops. The initial flux values were used as the starting values at the ZFE. The model treated the ambient field as having three layers each with a different stratification parameter $c = -gd\rho a/\rho_1 dz$. Layers 1 and 3 had no stratification, i.e., c = 0.

Integration of Eqs. 6-9 continued until the local momentum flux, Eq. 7, reached zero or the water surface was reached. The numerical solutions are plotted versus the experimental results in Chapter 5, Results and Discussion. A more indepth discussion of the numerical model is presented in Appendix A.

CHAPTER 4

EXPERIMENTAL APPARATUS AND PROCEDURES

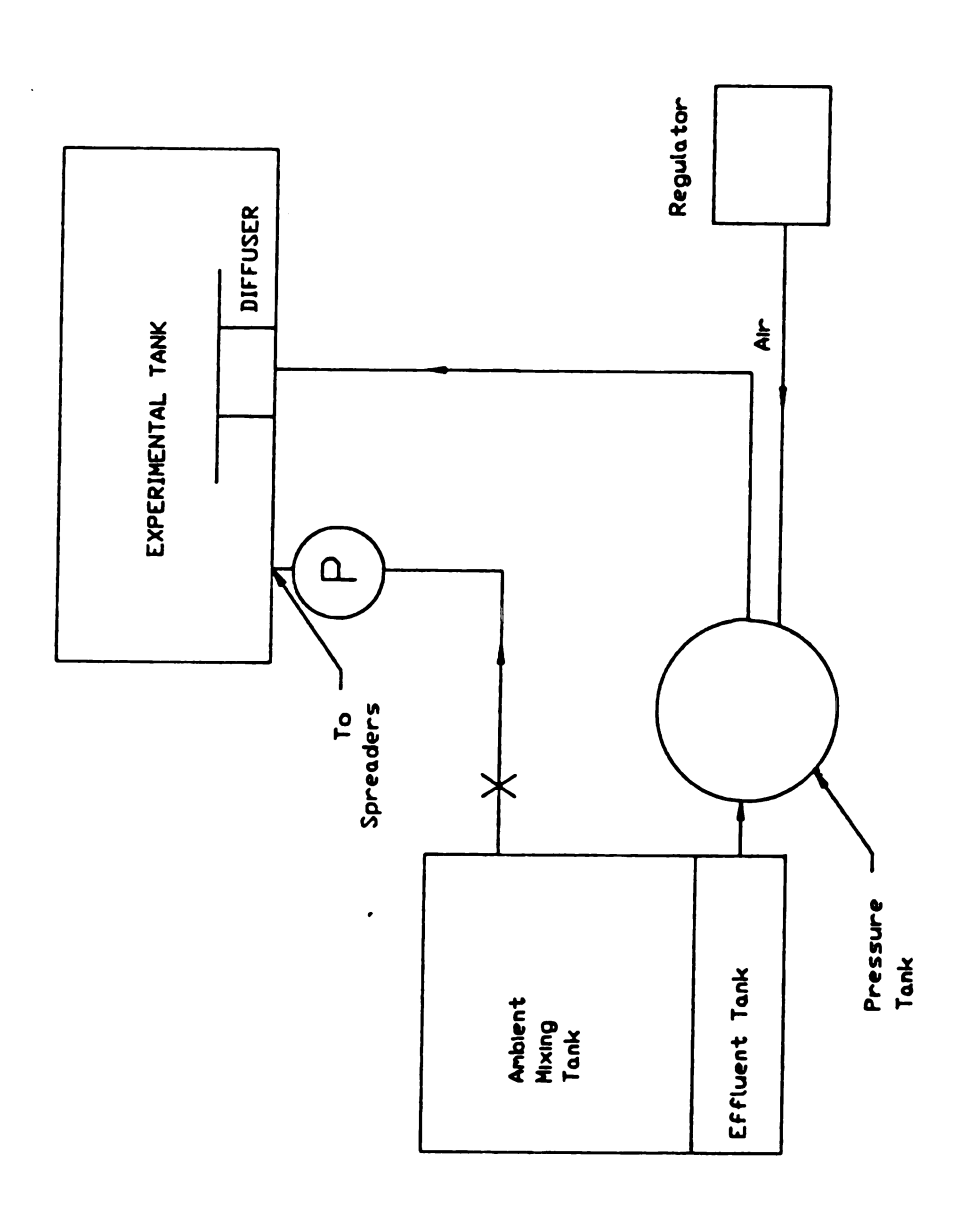
4.1 General

All experiments were performed in the first floor Structures
Laboratory, Engineering Building, Michigan State University campus. In
general, the experimental apparatus consisted of several wooden mixing
tanks and one larger experimental tank. In addition a jet diffusion
system, density determination equipment and a flourometer were
utilized. The general laboratory schematic is shown in Figure 9.

4.2 Tanks

Three plywood tanks were constructed for use in the experiments. The main experimental tank was 21' x 3' x 3' with a 5' x 3' acrylic window in one side. An intermediate wall was placed in this tank, 8 inches from the window and parallel to it (Figure 10). This wall effectively made the tank longer which increased the time the experiment could proceed. Fluid for the upper ambient layer was mixed in a separate 4' x 4' x 8' tank and then pumped to the experimental tank to develop the density stratification.

A small 1.5' x 4' x 4' tank was used to mix the salt, flourescein and water which comprised the test effluent. Once mixed, the effluent was transferred to a 120 gallon steel tank which held the effluent during the experiment. Once pressurized, this tank would maintain constant flow of effluent to the diffuser. This system is shown in Figure 11.



Plan of Experimential Laboratory

FIGURE 9

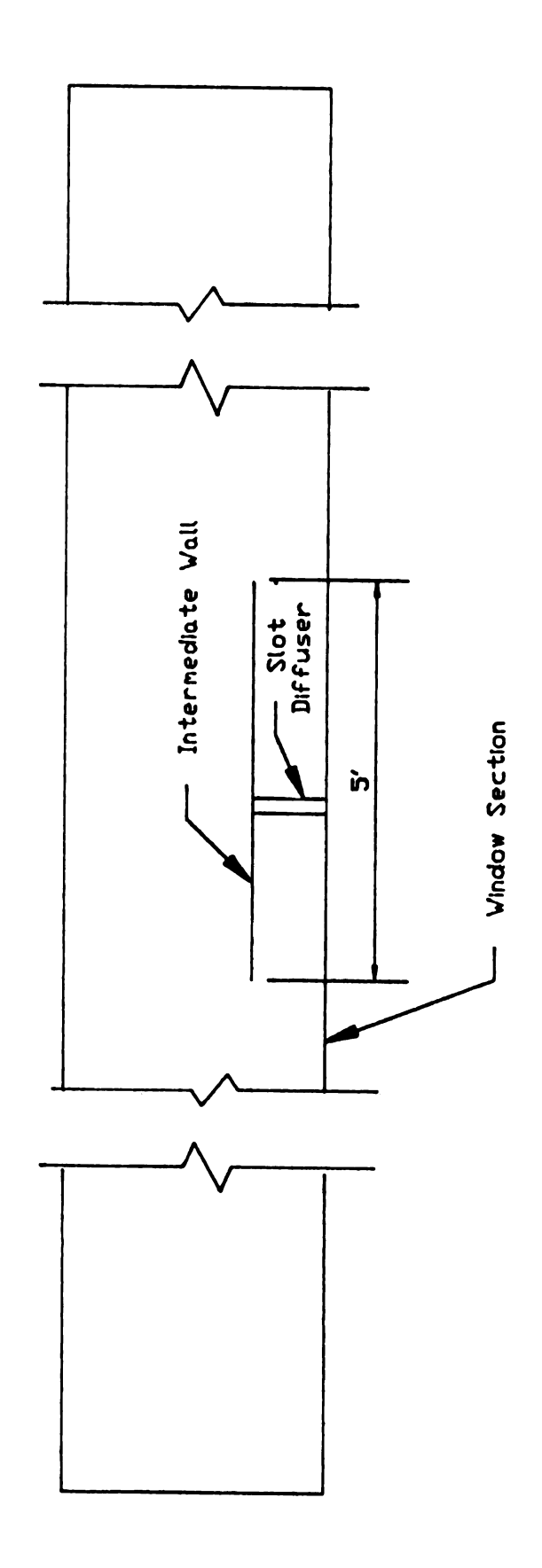
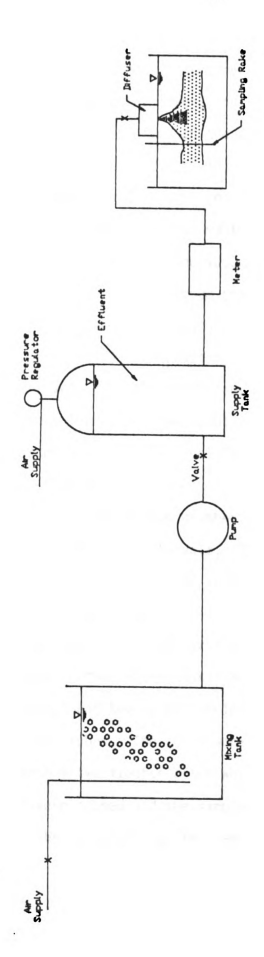


FIGURE 10

Plan of 21'x3'x3' Reservoir Showing Slot Diffuser Located Between Resevoir Window and Intermediate Wall,



<u>FIGURE 11</u> Schematic Diagram of the Jet Discharge System

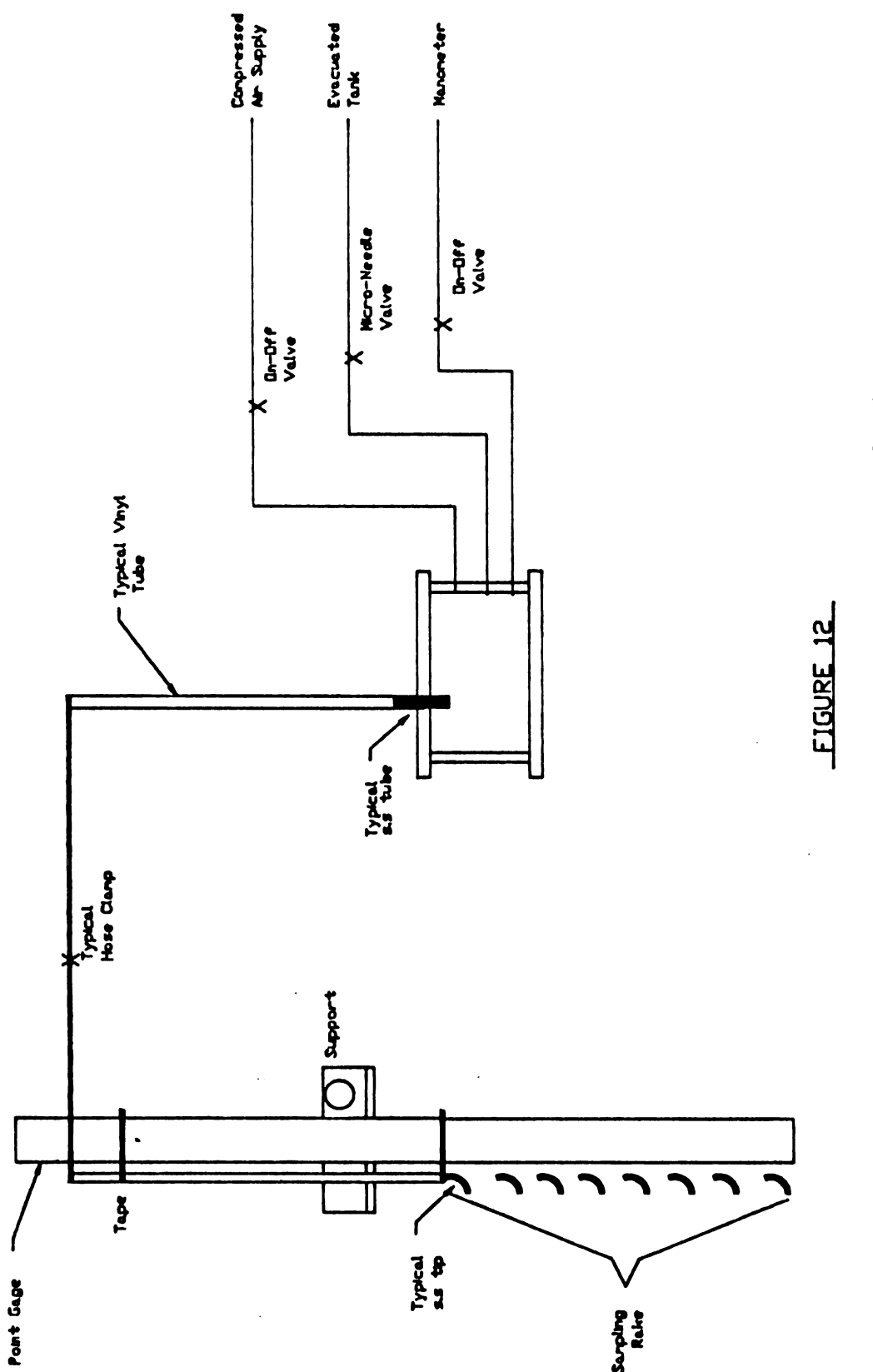
4.3 Suction Sampling System

Two suction sampling systems were used, one which collected samples from the effluent spreading layer, and another sampler for determination of the ambient density profile in the experiment tank.

The effluent sampler (Figure 12) consisted of a vacuum pump and tank, vacuum chamber, and a sampling rake. The vacuum pump was used to lower the air pressure in the vacuum tank. In turn, a micro-needle valve, placed in line between the vacuum tank and the suction chamber, was utilized to regulate the vacuum pressure in the vacuum chamber.

The vacuum chamber was constructed from an acrylic cylinder closed at each end (Figure 13). In addition to the vacuum line, also attached to the chamber were a pressure hose and regulator, a manometer, and the 20 sampler tubes leading to the sampling rake. The sample tubes were fabricated from model airplane fuel line and 0.125 inch stainless steel tubing. Flow in the sample tubes was controlled by screw-type hose clamps located near the vacuum chamber. The sampler tips were attached to a point gauge at 3 cm. intervals. The large number of sample points on the rake insured collection of sufficient data to understand the dilution variation with depth.

To operate the system, the pressure was first lowered to approximately -15 psig in the vacuum tank. Next hose clamps on the sample tubes were opened and the micro-needle valve adjusted to produce a slow flow through the tubes. The tubes were allowed to flow in this manner for approximately two minutes after which time the hose clamps and needle value were closed and the sampler withdrawn from the tank. The samples were then drained from the sampler lines into 5 ml. cuvetts.



Suction Sampling System for Collecting Dilution Samples from the Spreading Layer

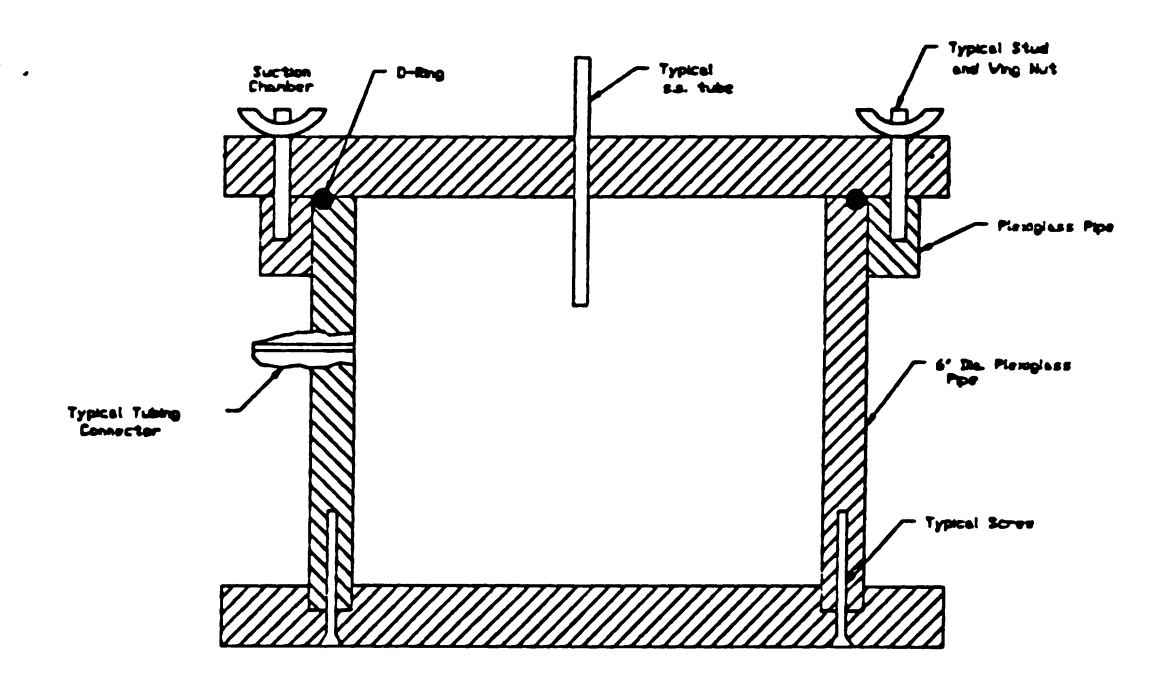


FIGURE 13

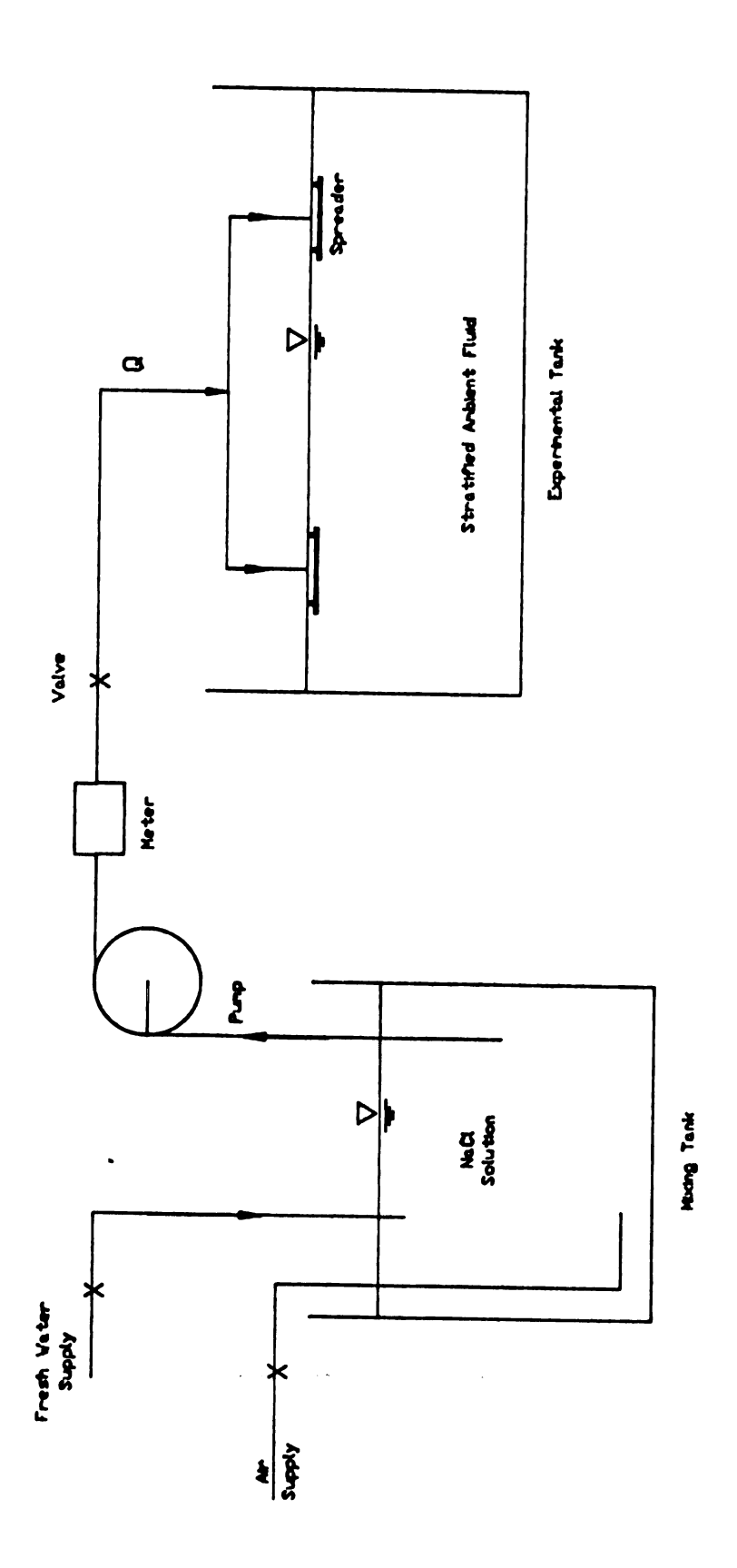
The Vacuum Chamber of the Suction Sampling System

The density profile sampler was used to withdraw ambient water samples near the interface between the two density layers. This system was identical to the dilution sampler except that no vacuum equipment was required and only a syphon withdrew the sampler from the tank. Seven stainless steel tips were connected to lengths of fexible tubing and mounted on a point gage. The tips were spaced at 0.25 inch intervals. Once the experimental tank was filled, ambient fluid samples from the interface were syphoned into beakers for fluid density determination. By sampling only one tube at a time (two if more than 1 inch apart), interference between sampling points was avoided. Sampling of the interface was continued until measured densities agreed with the grab samples taken of each layer before stratification began. In this way the desnity interface was bracketed by known density fluids. Usually, this entailed moving the sampler 1 inch up or down to collect sufficient data to completely bracket the interface.

4.4 <u>Stratification System and Density Measurement</u>

4.4.1 <u>Stratification System</u>

The purpose of the stratification system was to develop the density discontinuity in the experimental tank. The stratification system consisted of a pump, a PVC piping system with associated valving, and two plywood spreaders (Figure 14). The one-inch PVC pipe connected the mixing tank to the pump which in turn was attached to the flow spreaders located in the experimental tank. Each flow spreader was fabricated from 0.75 inch plywood, a one-foot section of 1.5 inch diameter PVC pipe, and two squares of fibrous packing material (Figure 15). The flow



Schematic Diagram of the Stratification System

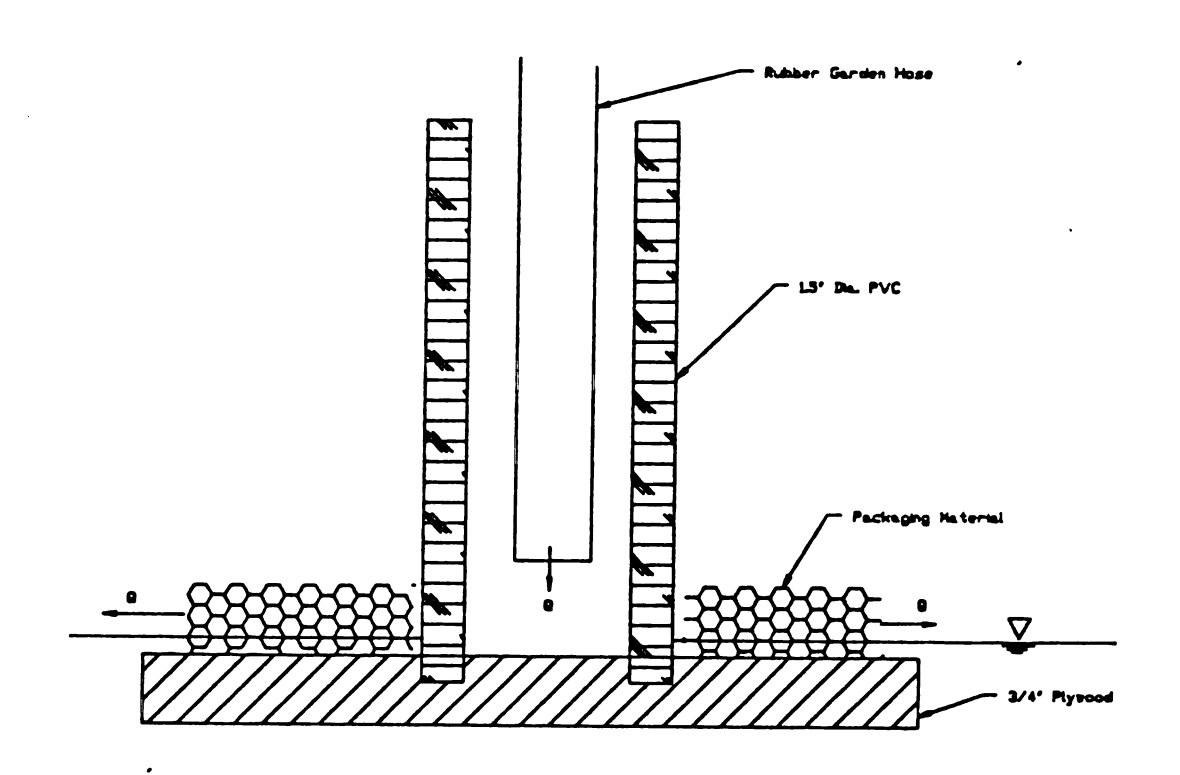


FIGURE 15
Flow Spreaders for Development of Two Layer System

spreaders were maintained approximately one-quarter inch below the water surface to minimize vertical mixing of the upper layer fluid with the lower layer fluid during the filling operation. The fibrous packing material was used to dissipate flow velocities of the salt water discharged from the holes in the 1.5 inch diameter pipe. To develop a stratification in the experimental tank, a small biforcation valve, downstream from the pump, was opened to permit a very low flow rate. , The first 5 centimeters of the upper layer fluid was placed at this initial flowrate. Next, the biforcation valve was opened halfway for the next 10-15 centimeters of fluid. Once 20 cm. of the upper layer fluid surface were in place, the biforcation valves were fully opened to finish filling the tank.

A simple, qualitative, flow visualization experiment was performed to determine optimum initial flow rates for stratifying. By coloring the lower layer, and using small grains of potassium premanganate to show flowlines at the edge of the spreader, the influence of the spreader location could be observed. These observations showed that flow rate had to be low as the top layer was spread over the heavier fluid. However, flow rate was not the only variable influencing the quality of the stratification. Waves, observed at the interface anytime a spreader was moved, caused the most significant vertical mixing. To avoid this problem the spreader was set to fill the first 5 cm. without adjustment. Furthermore, care was taken when working near the tank not to disturb the tank in a way that would produce waves.

4.4.2 Density Measurment

A specific gravity balance was utilized to obtain density measurements of the different fluids employed in the experiments. The Troemner model S-101 was chosen because of its reported high degree of accuracy, plus or minus 0.0001 gm/cm³. A dust and wind cover was built for the balance to eliminate interferences from the laboratory environment. A procedure was developed to insure the data collected were accurate and reproducible. An explanation of that procedure follows:

A sample of the fluid in question was decanted into a 200 milliliter glass test cylinder. Next, the sample was placed on the balance and the plummet was placed in the sample. At this point, the balance was released to the half point and a rough adjustment made. Next the balance was 75 percent released onto the knife edge and the fine adjustment chain was tapped to relieve any kinking that might have occurred. Finally the balance was released and find adjustment was made while the crossbar was swinging. When the displacement of the pointer on either side of center were equal, both plummet temperature and specific gravity readings were taken. A minimum of three weighings were performed on each sample and the average final weighing was calculated and used.

4.5 <u>Dilution Measurement System</u>

The dilution measurement system consisted of three parts: The suction sampler (see Samplers), the tracer dye (Flourescein-Yellow Uranine), and a Turner Model 111 Filter Flourometer. Since Flourescein can have its flourescense altered by many different constituents of the laboratory water supply, and because large decays were observed in some experiments, the chemistry of flourescent tracers was studied.

Variation of fluorescense concentrations with time, denoted by non-linearity of calibration curves or total loss of flourescense (color change), can be affected by several different conditions. Chemical causes include: free Chlorine, greater than 0.5 ppm, (Wallace, 1981) Bromine, Iodine, NHCOCH $_3$, NO $_2$, and COOH groups (Willard, 1981) or a drop in the ph of a system below 5.5 or a rise above 8.0 (Feuerstein, 1963). Physical causes include temperature increase and exposure to

ultra-violet radiation (Wallace, 1981). Finally, Flourescein can quench its own flourescense at concentrations greater than (10)-4M (Willard, 1981).

The water quality records for Michigan State University did not suggest that any of the chemical reasons were causes for the observed decays. Furthermore, DPD colorimetric titrations were performed on samples of laboratory water. These analysis showed concentrations of free chlorine between 0.25-0.40 ppm, below the 0.5 ppm limit. To check for ultra violet radiation interference, tests using water samples of known flourescense, half in dark and half in laboratory light, were performed. These tests did not yield any photochemical decay. The actual cause of decay was never demonstrated conclusively. It is hypothesized that the large organic molecules of the tracer might have absorbed the salt used to adjust density in the experiments. Therefore, at a certain point, governed by the concentrations of the salt and the Flourescein, the salt absorbtion might become so great that all flourescense is quenched. This absorbtion is much like the modified Fajan method used in analytical laboratories to determine chloride concentrations in water samples where the reduced flourescense acts as the indicator for chloride concentrations.

As stated previously, the Turner Filter Flourometer, Model 111, was utilized for measurement of flourescense. The flourometer was equipped with the 47B and 2A primary filters and 2A-12 secondary filters. This setup was recommended by the manufacturer and baring chemical decay provided highly reproducible linear calibration curves.

Measurements of the concentration or dilution of effluent in the spreading layer was initiated by withdrawing discrete water samples from

the spreading layer. These samples were then placed in the flourometer and the relative tracer concentration was determined. The flourometer was calibrated during each experiment using a series of dilutions. These series dilutions were mixed from grab samples of ambient and effluent water samples collected before the jet was discharged. Once the serial dilutions and the spreading layer samples had reached a common temperature the first set of flouresence measurements was made. Between 30 minutes and one hour later a second set of flouresence measurements were taken. The actual time interval between measurements was determined with the following equation:

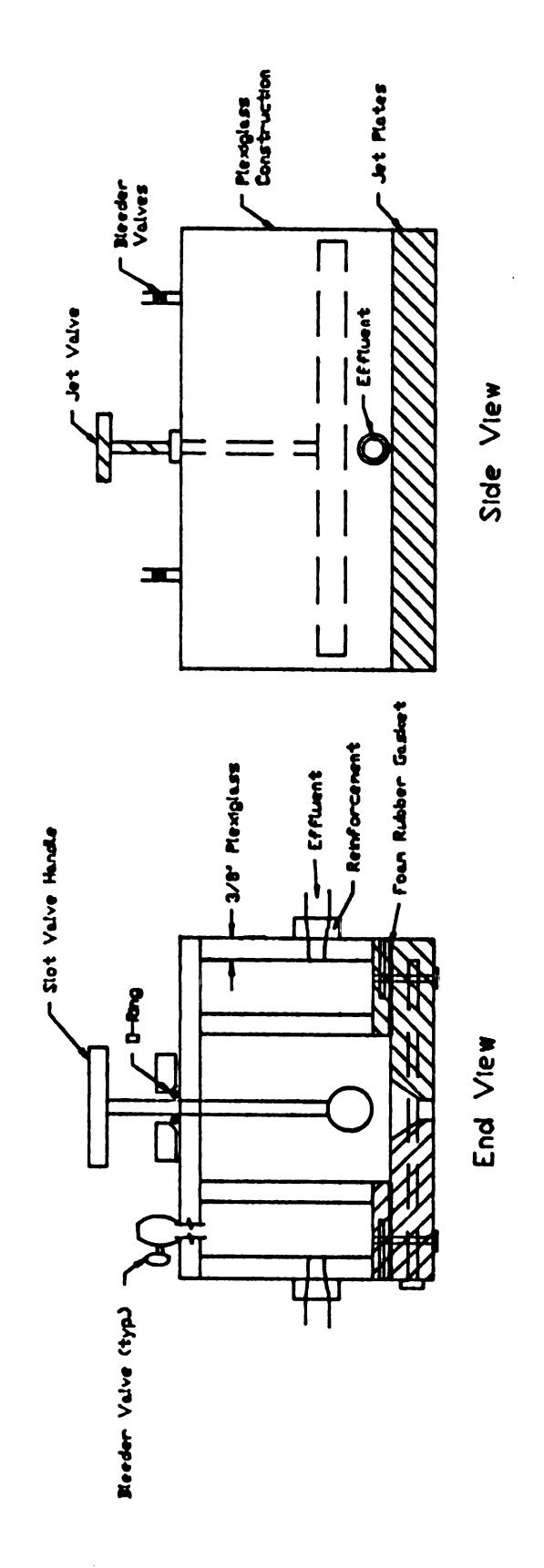
$$t_1 + (t_2 - t_3) = t_4$$
 Eq. 10

where, t_1 = the initial time when dilutions were mixed t_2 = the time when all samples and dillutions reached common temperature t_3 = time when the jet fluid began to mix with the ambient fluid in tank t_4 = time to take second flouresence measurement

The performance of double flouresence readings allowed an easy method to determine when slow changes in flouresence were occurring. These changes would be caused by something other than temperature since the temperatures were controlled during measurement. Tests which showed changes in flouresence of this nature were discarded.

4.6 <u>Diffuser System</u>

The clear acrylic jet diffuser system was modeled after the diffuser used by Wallace (1981), (Figure 16). Effluent was supplied to both sides of the diffuser through a hose and distributed along the jet length by baffles on either side of the jet slot. Air values were placed



<u>FIGURE 16</u> Schematic Diagram of Jet Diffuser System

on the top of the diffusers. The jet slot was formed by two, one-inch thick, uniformly milled, aluminum plates. Milled spacers were used to fix the slot size which could be varied from 0.15 to 1.15 cm. Bolts at both ends of the aluminum plates were used to draw the plates against the spacers. The slot thus formed was then bolted to the bottom of the diffuser. A foam rubber gasket made a seal with the diffuser. The jet slot was closed with a valve from the top of the diffuser while the diffuser was filled with effluent prior to the experiments. Flow rates thru the diffuser were measured with a Rotometer. The diffuser and jet slot were built by the students of the Utica High School Machine Shop, Utica, Michigan (Instructors: Mr. Tony Buchannan and Mr. Alvin Sheff) and by the Michigan State University Engineering Machine Shop.

To produce a plume the diffuser slot was closed with the valve and the air bleeders opened. The supply tank was pressurized and the supply valve opened. Air was then bled from the side baffle areas until the entire diffuser was filled with effluent. At this point the air bleeder valves and all valves controlling flow were closed. The entire system was checked for leaks. Effluent leakage from the diffuse was allowed to spread away from the viewing area. Then the diffuser slot valve and supply valves were opened together and the flow adjusted to the predetermined rate.

4.7 Procedures

The overall procedure for an experiment with a two-layer ambient stratified is explained below. Details of certain steps are described in the sections which discuss the various pieces of equipment. The tanks were rinsed from the previous day's experiment and the supply lines were

flushed approximately 30 minutes. Free chlorine concentrations in the supply water was measured to insure that the concentration was less than 0.5 ppm. While the lines were being flushed, the experiment was selected and the values of variables which had to be controlled were calculated.

Once cleaned, water for the heavy layer was added to the experimental tank. Salt was added and forced to mix until a uniform density was achieved. The specific gravity of grab samples from several locations in this layer were measured to determine that the layer was homogenous. With the heavier layer in place, the lighter layer was mixed in the same manner in the mixing tank. Finally, water, salt, and tracer were mixed in the small mixing tank to make the effluent. Once mixed, the effluent was transferred to the jet supply tank.

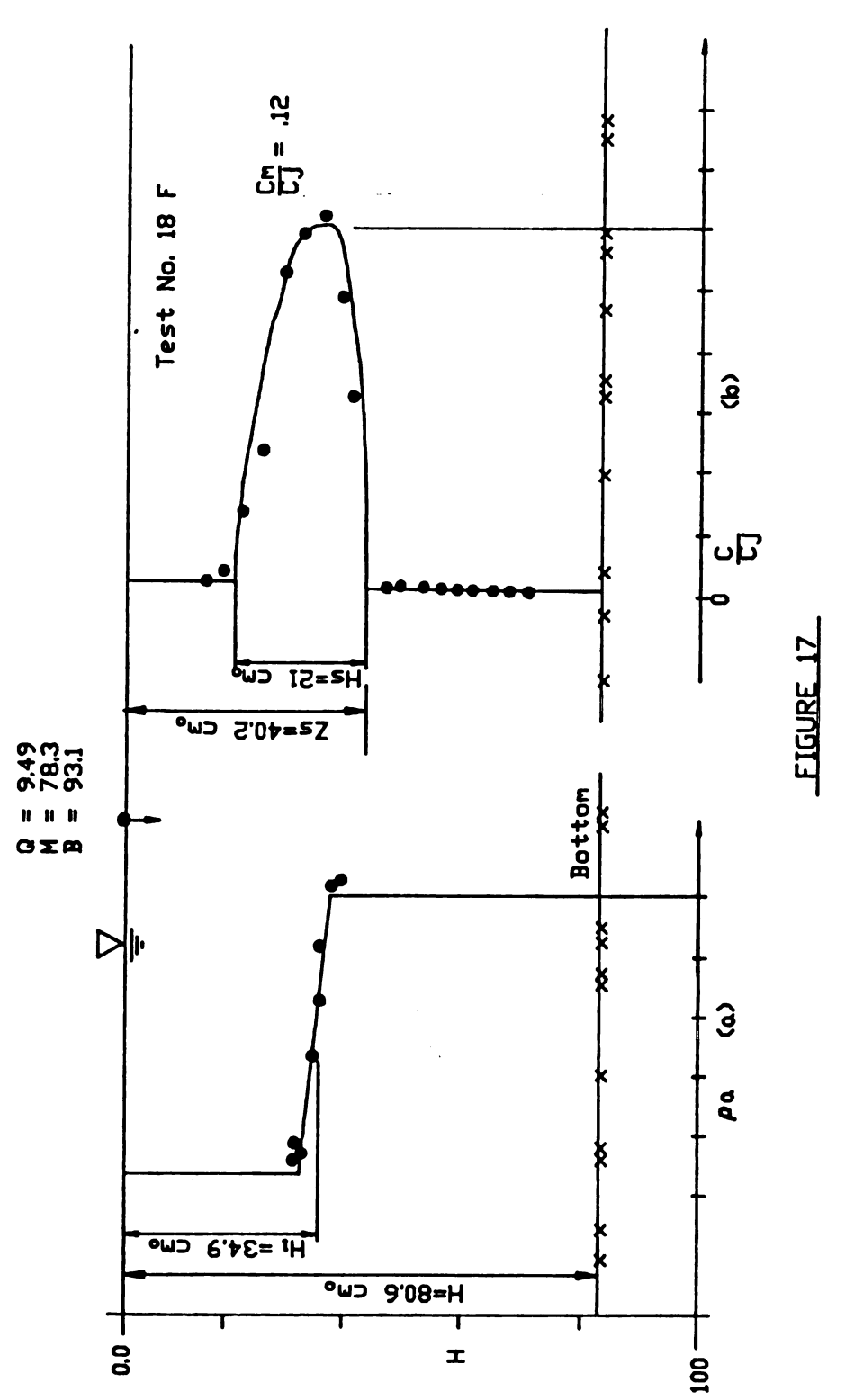
Once the heavy and light fluids were prepared, the experimental tank was stratified. During the stratification process, the jet fluid was sampled and its density was measured, the suction sampler cleaned, the slot width was adjusted and measured, and the suction sampler was readied. When the experimental tank was full, samples from the stratification interface were withdrawn and weighed. Finally, the suction samplers were positioned and the initial depth of each sampler was measured.

In the last minutes prior to starting the jet, ambient and effluent grab samples were collected and T1, T2 and Tj were measured. The experiment number was noted on the side of the tank and the diffuser was connected and bled. When any jet leakage had dissipated, the time was recorded, the diffuser opened, and the correct effluent flow set. The flow meter was read a minimum of three times during the experiment. Once the spreading layer developed, both the sample tubes and the needle valve

were opened to allow the vacuum to draw samples. The sampler was allowed to run for approximately two minutes to insure a time averaged sample from the spreading layer. In addition, photographs were taken and any interesting facts regarding the experiment were noted. Finally, the maximum height of rise, Zm, was marked on the observation window.

When all spreading layer samples were collected and measurements made, the supply valve was closed and the tank drained. The flourometer was turned on, and the series dilutions were made and allowed to come to a common temperature. Once a common temperature was reached, the spreading layer samples and series dilutions were placed in the flourometer and readings were taken. While waiting for the caculated lag time to elapse, a calibration curve was drawn to check for large, early decays. Last, Zm was measured on the basis of the position of the maximum rise that was recorded on the lucite window.

An example of data collected for a typical experiment is presented in Figure 17. Part A of that figure shows the measured stratification interface. The lighter layer thickness, H1, is taken as the distance from the jet origin to the midpoint of the density gradient. The density gradient midpoint was found by first adjusting all stratification data to the temperature of ambient fluid during the experiment. Then, the midpoint was simply read off the graph of the density gradient. The minimum dilution, Sm, was determined as the inverse of the maximum relative concentration in the spreading layer. Table 1 presents a summary of all experimental data collected.



a) Typical Variation of Ambient Density with Elevation Before Experiment,

b) Typical Variation of Effluent Concentrations Measured in Spreading Layer.

					Table 1	-						
Experiment No.	Cm ² sec	o (ma)	(ဏ)	g'g (m) (sec²)	g' (cm 2)	H, (m)	н (шэ)	(m)	(m)	* _% E	h _s (ma)	(cm)
7	6.14	0.86	18.14	21.8	23.9	41.9	80.5	2.80	44.	14.2	22.0	44.2
2F	5.05	0.86	18.14	26.1	9.61	37.3	80.5	1.60	46.0	15.7	19.0	41.8
3F	4.95	0.86	18.14	8.74	25.8	38.9	80.5	1.30	42.0	10.7	18.0	40.8
4F	4.94	0.86	18.14	8.35	8.84	38.1	80.5	1.70	41.0	12.0	16.5	41.1
6F	4.88	0.86	18.14	20.4	1.47	40.8	80.5	6.70	80.5	17.4	50.5	90.6
9F	5.00	0.86	18.14	3.46	0.0	:	90.6	:	90.6	17.2	33.0	90.6
16F	20.2	1.11	18.02	34.6	5.06	35.6	90.6	1.70	90.6	13.3	33.5	90.6
17F	10.5	1.15	18.02	11.9	3.04	37.3	90.6	3.3	74.0	9.3	30.0	52.2
18F	9.49	1.15	18.02	9.81	4.61	34.9	90.6	4.00	49.9	8.3	21.0	40.3
19F	10.0	1.15	18.02	24.1	2.84	37.5	90.6	1.00	90.8	20.0	59.3	90.6
20F	9.84	1.15	18.02	23.4	3.04	35.0	90.6	2.90	90.6	15.6	52.0	77.5
61583	5.16	0.31	18.00	14.7	0.0	;	81.0	;	81.0	23.9	31.0	9.08
62383	2.07	0.86	18.14	14.4	0.0	:	90.08	1	90.08	30.3	26.5	9.08
62883	5.20	0.86	18.14	22.4	0.0	;	90.6	:	90.6	32.2	25.5	90.6
121583	19.23	1.15	18.02	27.3	11.1	36.5	80.8	3.11	64.1	8.47	33.0	50.0
121683	13.70	1.15	18.02	18.7	5.10	35.8	80.5	6.73	80.5	8.93	29.25	52.0
122083	16.53	1.15	18.02	28.5	3.63	33.3	80.5	3.43	80.5	8.40	60.5	80.5
122183	14.56	1.15	18.02	22.2	2.26	35.6	90.6	2.86	80.6	11.36	38.5	90.6

* Dimensionless

CHAPTER 5

RESULTS AND DISCUSSION

5.1 General

The primary objective of this study was to quantify the behavior of buoyant waste plumes discharged into ambient fields with non-linear density profiles. Based on the experimental data, dimensionless numbers were calculated utilizing previously developed equations, which characterized different ambient and effluent conditions. Graphs of the stratification strength, $\frac{\text{Hig}^4}{\text{B2/3}}$, versus the dimensionless forms of Zm, Hs, Sm, Zs were then used to determine the equations predicting plume behavior.

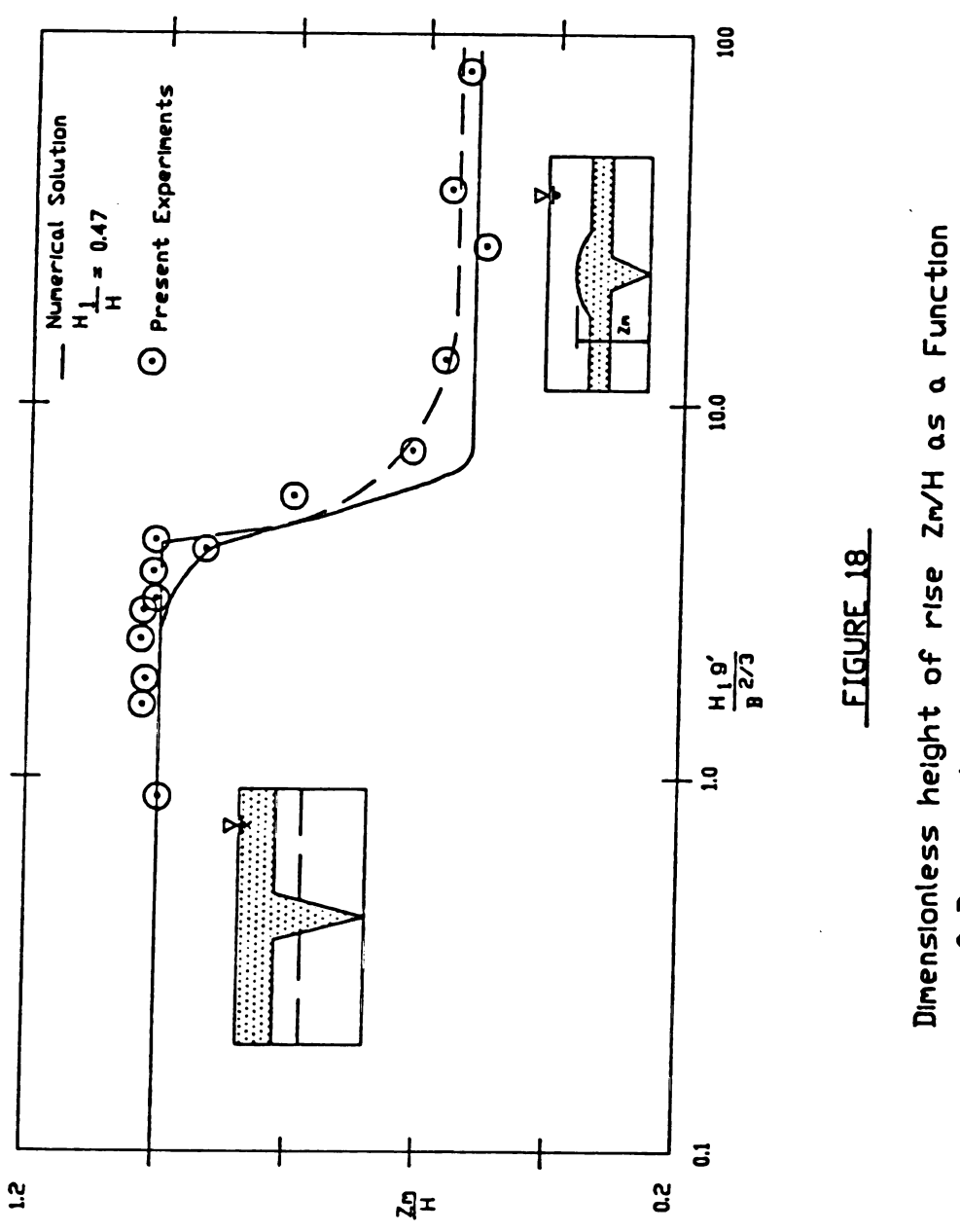
5.2 Maximum Height of Rise

The values of Zm, the maximum height of rise, were measured during the experiments. In addition, utilizing the independent experimental values, the numerical model was utilized to predict the value of Zm.

Figure 18 represents the numerical and experimental results of the maximum height of rise, Zm. The measured data yields the following asymptotic equations:

$$\frac{Zm}{H}$$
 = 1.0 $\frac{H10'}{B^{2/3}}$ < 4.7 Eq. 12 $\frac{Zm}{H1}$ = 1.08 $\frac{H1g'}{B^{2/3}}$ > 1.5 Eq. 13

These equations are correct with less than 10 percent error in the given ranges of H1g/ . These equations do not represent the rise from H1 to H in moderate stratifications which occur in the transition zone



Dimensionless height of rise Zm/H as a Function of Dimensionless Strength of Density Discontinuity $\rm H_1\,9/B^{2/3}$

1.5 < H1g'/B^{2/3} < 4.7, although values are very well predicted either side of this zone. The location of this transition zone for moderate stratification is reasonably well predicted by the numerical results, although the numerical results do not show the beginning of the rise into the upper layer at as large a value of $\frac{\text{H1g'}}{\text{B2/3}}$ as experimentally

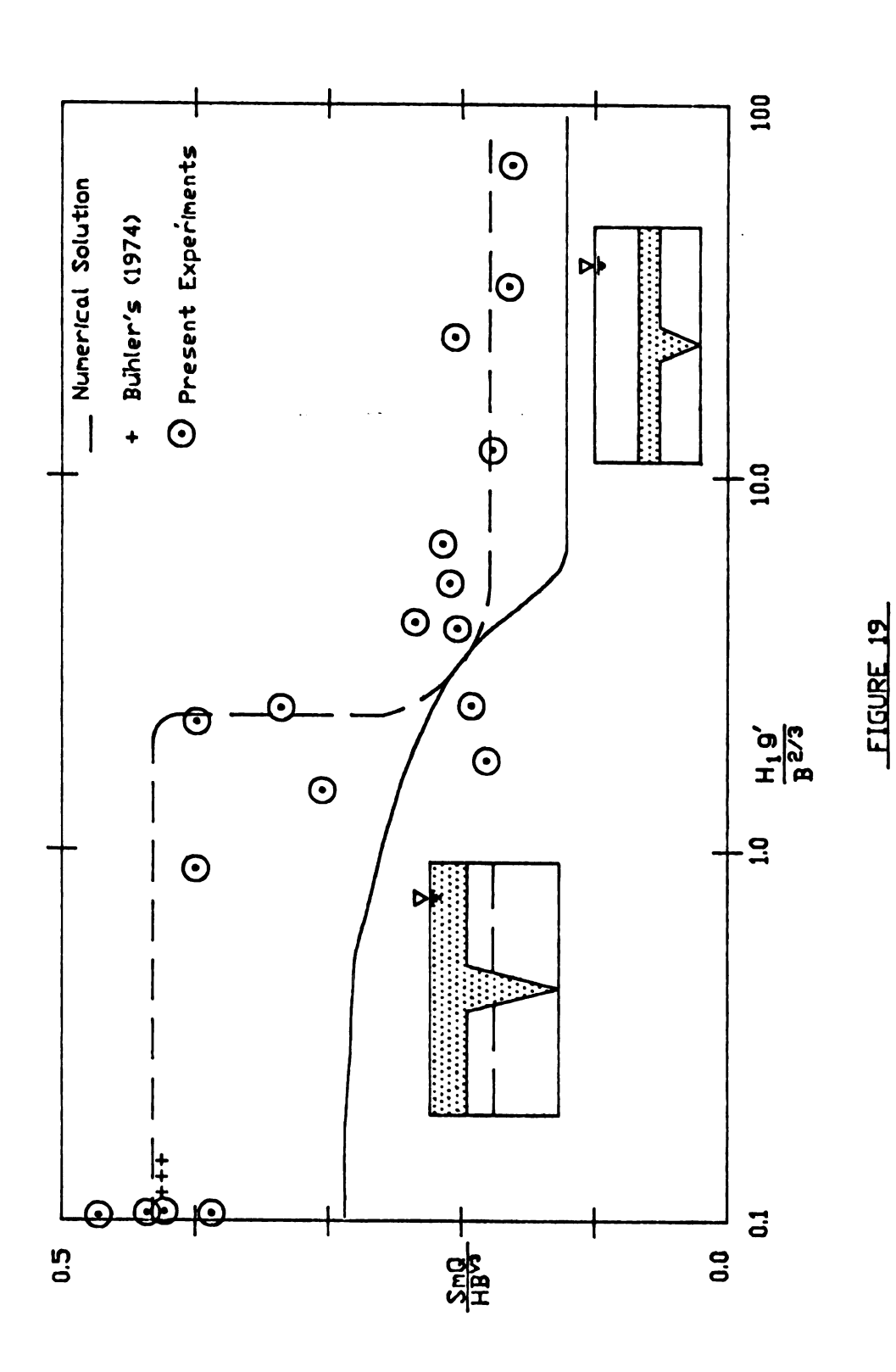
observed. The numerical results of maximum rise agree well outside of the moderate stratification region. In the region where Zm is less than the full depth, H, the H parameter has no physical meaning. However, it does have a bearing on the plotting position of the specific experiment because scaling is performed by H, not H1. Therefore, all data in the preceeding scenario, and the following scenarios were adjusted to reflect the ratio of H1/H = 0.47. In this way, the correct uncertainty in the data is shown.

5.3 Minimum Dilution

The values of Sm, the minimum dilution, were measured during the experiments. In addition, the numerical model was utilized to predict the values of Zm from experimental data. Figure 19 represents the experimental and numerical results for the minimum dilution, Sm. The dimensionless asymptotic solutions can be estimated with less than 10 percent error as in the ranges indicated:

$$\frac{\text{SmQ}}{\text{HB} \, 1/3} = 0.42$$
 $\frac{\text{H1g'}}{\text{B} \, 2/3} < 2.4$ Eq. 14
 $\frac{\text{SmQ}}{\text{H1B} \, 1/3} = 0.42$ $\frac{\text{H1g'}}{\text{B} \, 2/3} > 3.8$ Eq. 15

Aside from the variation in measured values due to experimental uncertainties, this relationship is excellent and only presents problems in the



Dimensionless Minimum Dilution as a function of Dimensionless Strength of Density Discontinuity $H_1g'/B^{2/3}$

range from 2.4 < $\frac{\text{Hig'}}{\text{B2/3}}$ < 3.8, the transition between the H1 to H rise.

This transition range represents the only problem area of the experiments. It could be caused by the constraints of the experimental setup or a still unknown plume characteristic. This area produced the thickest spreading layers (up to 80 percent of the total depth).

The numerical results predict 25-35 percent less dilution than actually occurred. It is not believed that this is caused by entrainment that occurs when the jet fluid spreads to the sampling point. The numerical results show a much broader transition region than measured or seen in the numerical results for Zm. This occurs because the integral equations model entrainment in such a way that dilutions can be increased beyond what occurs when Zm first reached H as $\frac{\text{Hig}^4}{\text{B2}/3}$ is reduced from larger values. The additional dilution occurs because Zm can go to H as soon as $\frac{\text{Hig}^4}{\text{B2}/3}$ gets small enough to allow a small but positive buoyancy flux in the layer above the interface. At the transition point, and smaller values of $\frac{\text{Hig}^4}{\text{B2}/3}$, the entrainment model predicts reduced entrainment and therefore dilution, whereas continued increase in the local buoyancy flux as the plume enters the top layer physically increases the entrainment in this layer without the possibility of increasing Zm.

Current experiments performed in homogenous ambient fluids were plotted at the point where $\frac{H1g'}{B^2/3}$ equals 0.1 so they could be placed on the graphs. Measurements in the present study are in excellent agreement with those of Buhler (1974). Buhler's experiments used a multi-port diffuser to discharge a plume into a weak two-dimensional current.

5.4 Spreading Layer Height

In Figure 20, the experimentally determined values of spreading layer height, Zs, are represented. The dimensionless heights are characterized by the following asymptotic solutions:

$$\frac{Zs}{H}$$
 = 1.0 $\frac{H1g^{1}}{B^{2}/3}$ < 2.80 Eq. 16
 $\frac{Zs}{H1}$ = 1/05 $\frac{H1g^{1}}{B^{2}/3}$ > 8.0 Eq. 17

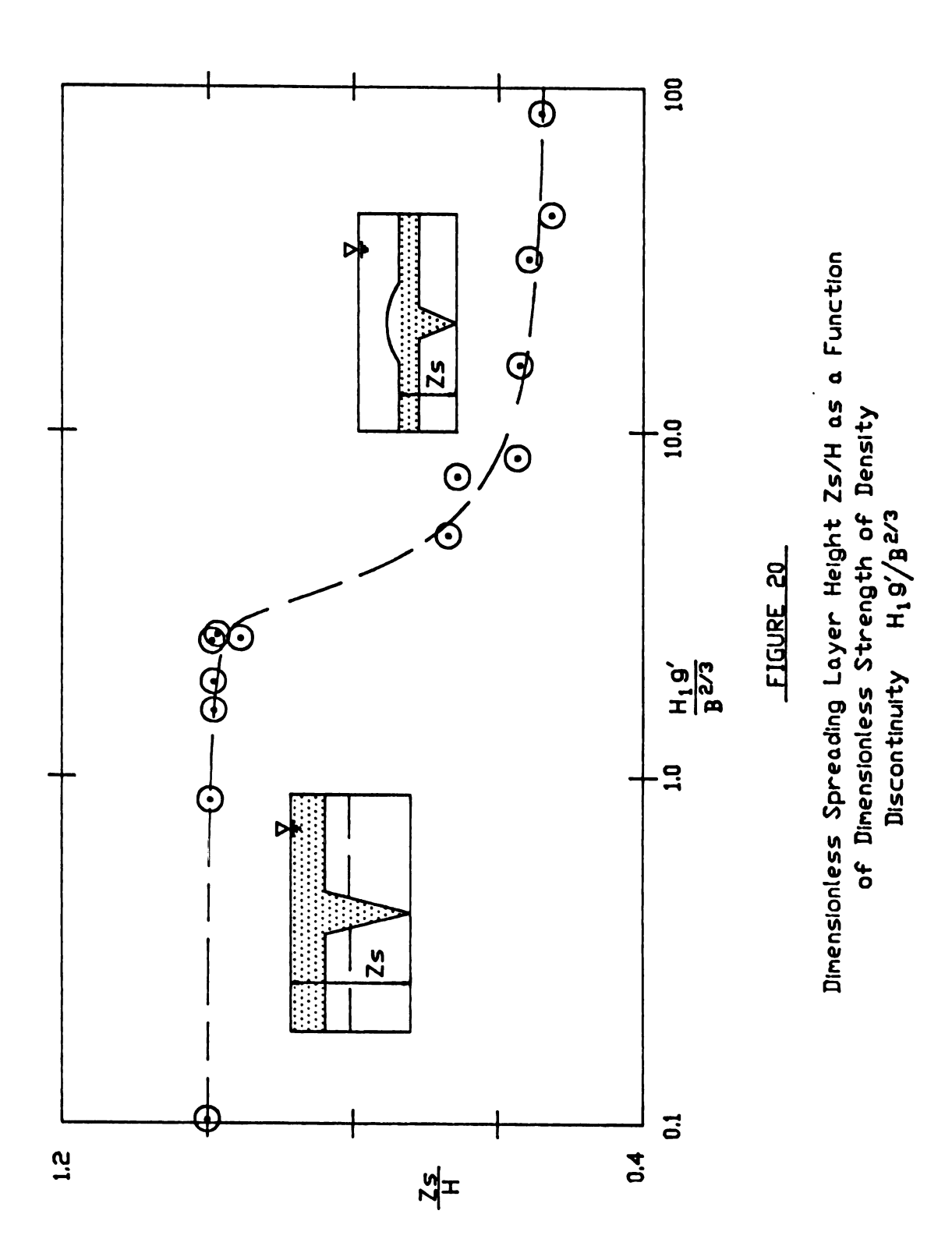
These equations can be used to cite the spreading layer with less than 10 percent error in the given ranges. Spreading layer heights in the transition region can be estimated using Figure 13 with the same error. The coefficient of Zs/H1 is greater than 1.00 because the plume centerline could always rise past the center of the stratified area. Data in the transition range show that fluid can spread in the region above the interface and still below the surface.

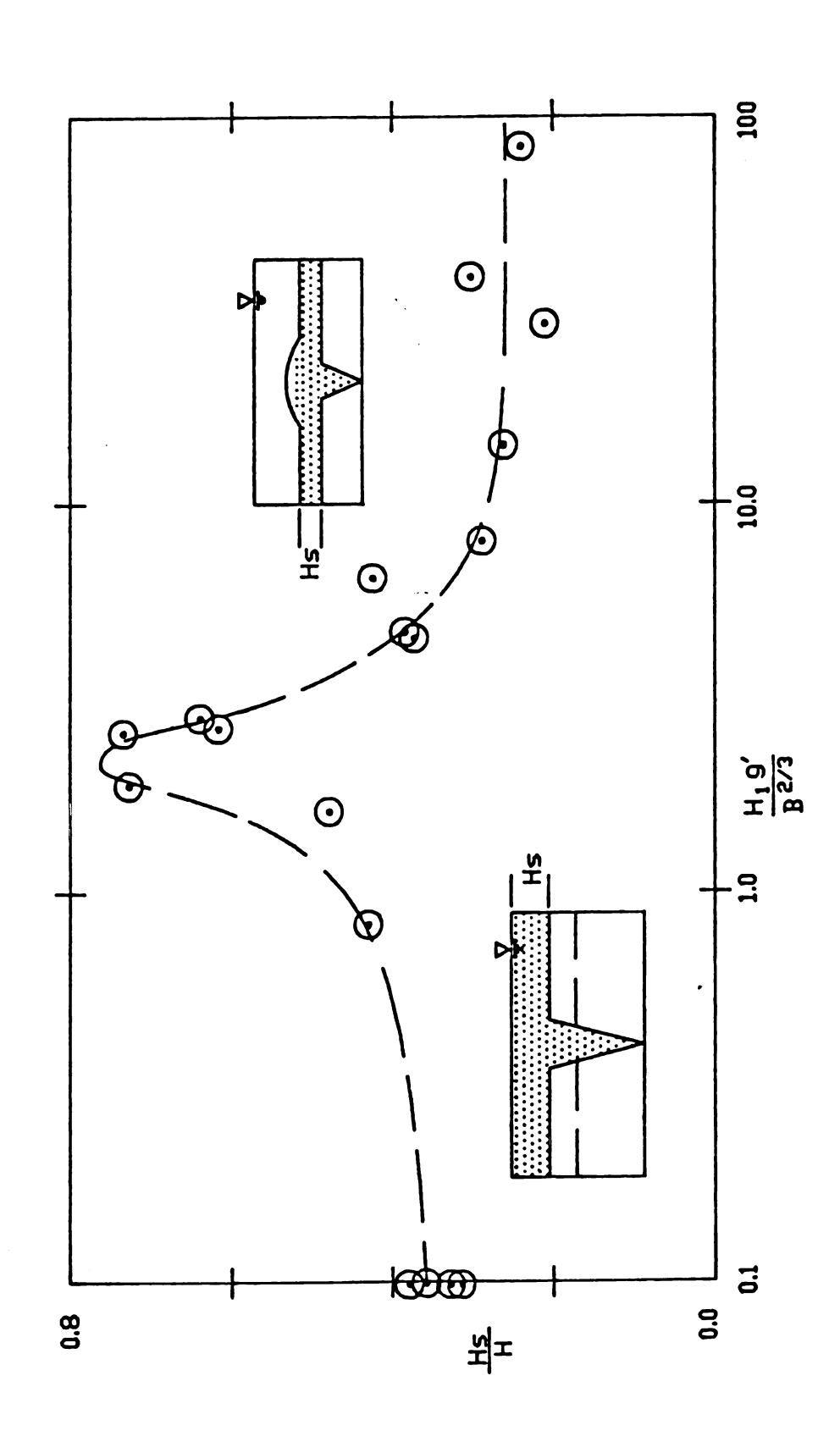
5.5 Spreading Layer Thickness

Figure 21 represents the experimental dependency of the spreading layer thickness, Hs, on the stratification strength. This graph yields the following equations:

$$\frac{\text{Hs}}{\text{H}} = 0.37$$
 $\frac{\text{H!g'}}{\text{B2/3}} < 1.0$ Eq. 18
 $\frac{\text{Hs}}{\text{H}} = 0.48$ $\frac{\text{H1g'}}{\text{B2/3}} > 8.0$ Eq. 19

These equations can be used with less than 10 percent error. The scaled thickness of 0.37 for the weak stratification class compares well with similar measurements in homogenous ambient fields as reported by Roberts (1977) who states that his, Liseth's, and Buhler's measurements indicated dimensionless thicknesses of approximately 30, 30 and 40 percent,





Dimensionless Spreading Layer Thickness Hs/H as a Function at Dimensionless Strength of Density $H_1\,9/B^{2/3}$

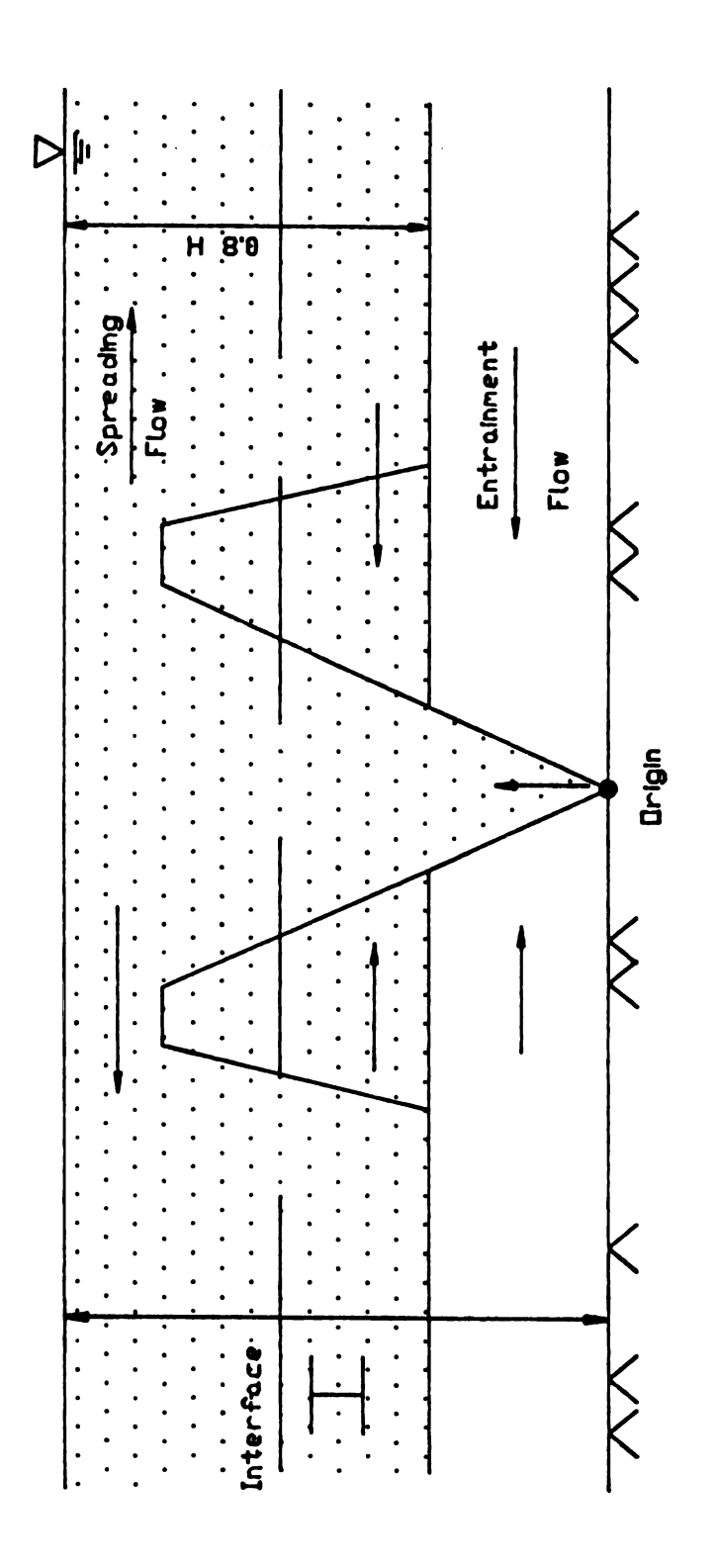
FIGURE 21

respectively. The constant in Eq. 18 is not identical to that of Eq. 19 because the density interface had a finite thickness on the order of T/H1 = 0.071 and was never strong enough to stop the fluid from mixing a small amount into it. This is different than the water surface which can stop plume rise completely.

The peak in spreading layer thickness at 80 percent was assumed. Although the maximum possible value would be 100 percent, it is not known if the demand for entrainment fluid near the jet origin is strong enough to pull effluent from the spreading layer (see Figure 22). This is more a question of stratified flows and will not be addressed here.

5.6 Summary

All of the data presented suggest a transition zone which has some very unusual features. Some plumes which could initially penetrate the full thickness, H, fell back to spread at the interface. Other plumes in this region would rise to H and spread but also fall back through the interface and spread over a thickness greater than H - H1. A reason for this could be that the momentum generated in the rise to the interface causes the slightly heavy plume to continue to rise to the surface. But the plume will than fall back to its neutral position. Another feature of this region is the entrainment of tracer by the rising plume. Qualitative experiments with different color tracers showed horizontal velocities towards the rising plume in the area immediately above the interface in addition to entrainment at the jet origin, Figure 20. This was observed in the plumes which spread to fill more than 70 percent of the total depth. When these experiments were allowed to run an extended period, the entire spreading layer would eventually fill the entire depth H and act as a plume in a homogenous ambient field.



Maximum Spreading Layer Thickness

CHAPTER 6
CONCLUSIONS AND RECOMMENDATIONS

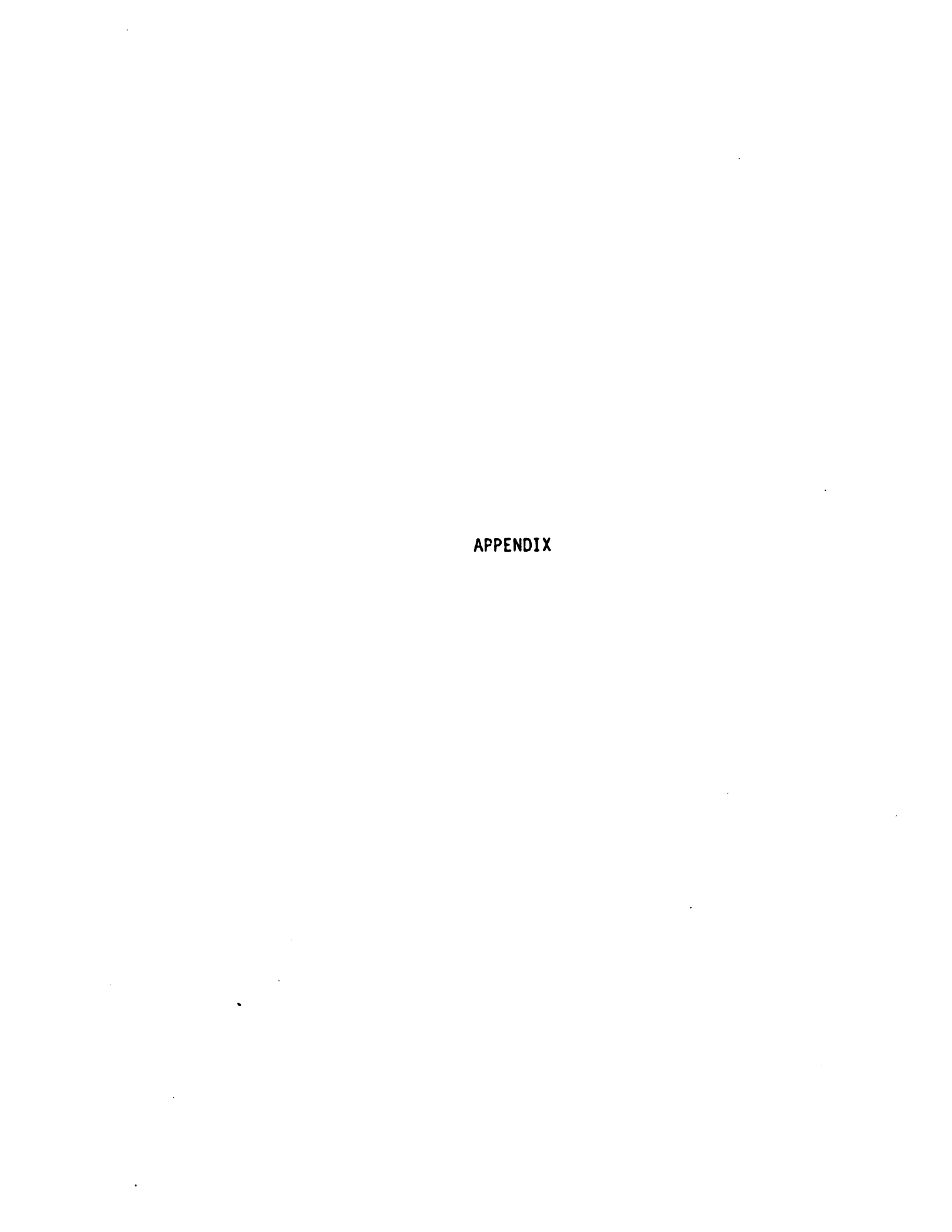
A study was performed to quantify the behavior of effluent plumes discharged into ambient bodies with non-linear density stratifications. Dimensional analysis was used to predict plume behavior under different ambient and effluent conditions. The following equations (Table 2) were determined for the parameters of minimum dilution, Sm, maximum rise, Zm, spreading layer thickness, hs, and spreading layer height, Zs. All of the equations in the table can be used with less than 10 percent error.

Table 2

Parameter	Parameter Value	Stratification Strength Bound	Eq.
Zm H		< 4.7	12
Zm H1	1.00	> 15	13
Sm0 HB1/3	0.42	< 1.5	14
SmQ H1B1/3	0.42	> 3.8	15
Zs H	1.00	< 2.80	16
Zs H1	1.05	> 8.0	17
Hs H	0.37	< 1.0	18
Hs H1	0.48	> 8.0	19

A numerical program was written to determine the minimum dilution and the maximum rise. A transition region was found where Eqs. 12 through 19 do not accurately predict observed behavior. In situations where design is required in the transition region, the figures which present the experimental data should be utilized.

More experiments are needed to better define the transition ranges. A different experimental setuup might be needed that would allow a much larger H value. A longer window might also be added to see if the observed behavior in the transition zone was actually in the main plume instead of the spreading layer. When the region is better defined, the numerical model could be updated to include the parameters of Zs and Hs.



APPENDIX A

This appendix includes a cursory summary of past numerical models. In addition, the model B-JETL will also be presented with a listing of the source code and example input and output.

Past Models

Available numerical models estimate the maximum rise and dilution produced by buoyant jets discharged into a ambient body. The most general of numerical models in a linear stratification is that of Fan and Brooks (1969). For non-linear stratifications Schatzman's (1977) and Sotil's (1971) models are available. All of these models make the assumption that velocity, tracer concentration, and buoyancy have similar (Gaussian) profiles over the jet width. This is invalid at the spreading layer because of the blocking that the layer causes. Also, entrainment assumptions are made because this parameter has not been determined for stratified fields or when spreading occurs. Brooks (1972) recommended that more laboratory research be undertaken to verify numerical slot buoyant jet solutions.

Program B-JETL

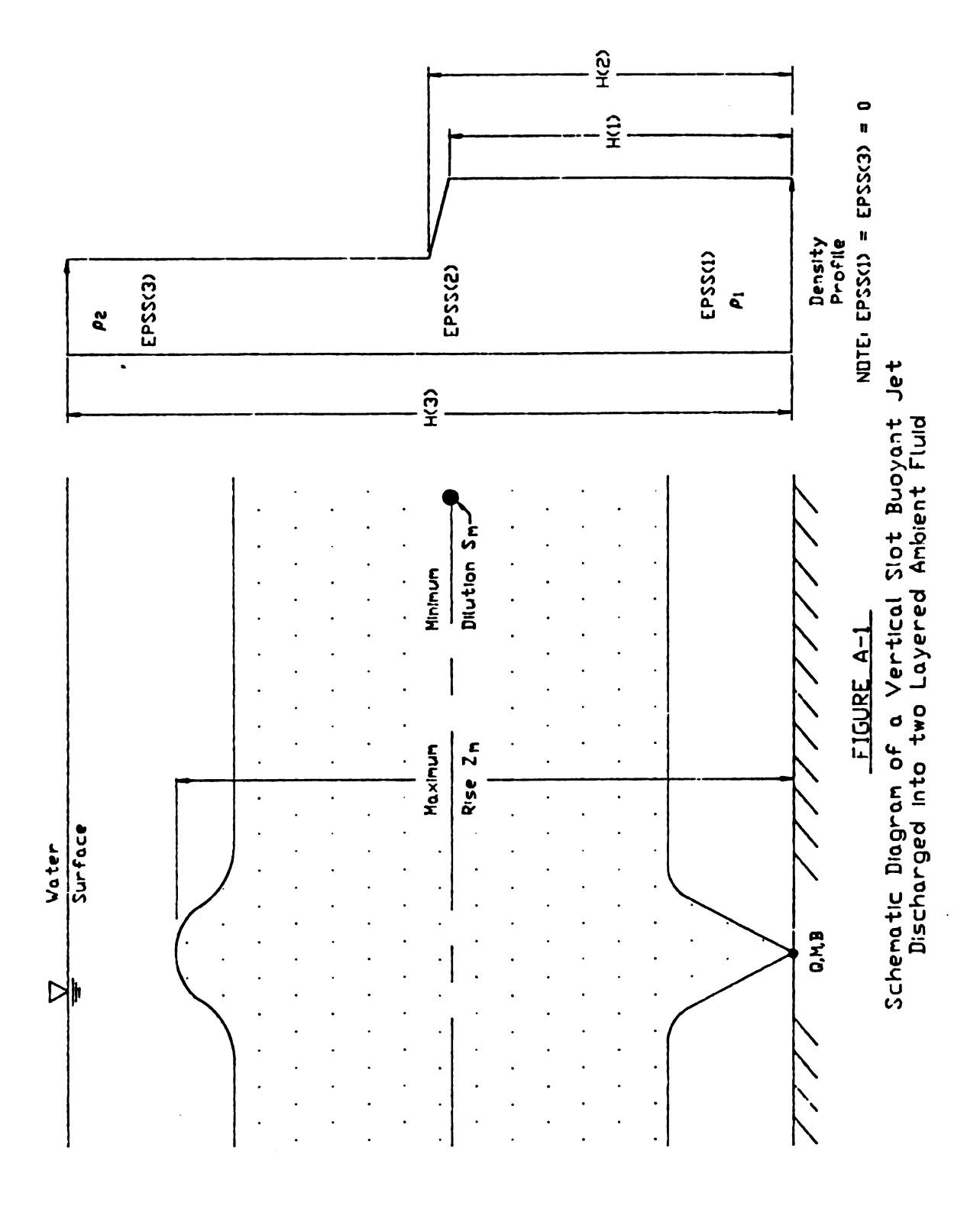
Program B-JETL determines the minimum centerline dilution and maximum rise for slot buoyant jets vertically released in a three-layer environment (in calling the environment three-layer instead of two, the assumption is made that the thermocline has a finite width). The program is written in Fortran 5 and was run on the Cyber 750 at the Michigan

State University campus. A commercial differential equation solver was used to integrate the descriptive equations. This equation solver used the Runga Kutta-Verner fifth and sixth order method with automatic error control. The integration begains at a distance $z=5.2\ Q^2/M$, which is the end of the zone of flow establishment. The terminal height is the z value where the momentum flux was zero, or the water surface, whichever is encountered first. The dilution calculated at this point is taken as the minimum dilution.

Input are the initial fluxes of volume, momentum, and buoyancy. The ambient stratification is described by the distance from the jet origin to the top of each layer and each layer's stratification parameter $\varepsilon = -gd\rho a/\rho dz$. In the present application, the first and third layers had uniform densities ($\varepsilon = 0$). Values of the entrainment, either the Morton or List and Imberger assumptions, and the tolerance for each integration step were also input. Output are the fluxes of volume, momentum, buoyancy, and dilution at values of z ranging from the beginning of established flow to terminal height.

A schematic diagram of a vertical slot buoyant jet is presented in Figure A-1. Fan and Brooks (1969) analyzed two-dimensional buoyant jets in linear stratifications. Their analysis used the Mortan type entrainment (E = $2\alpha w$) to obtain the differential equations describing the problem. To integrate these equations, the following assumptions were made:

- 1. The fluids are incompressible.
- The Boussinesq assumption was made that variations of density throughout the flow field are small relative to the reference density chosen.



- 3. The fluid density is assumed to be a linear function of salt concentration or temperature.
- 4. The jet is fully turbulent; therefore, no Reynolds number dependency occurs and the molecular diffusion is small compared to the turbulent transport.
- Longitudinal turbulent transport is small compared to longitudinal advective transport.
- 6. The pressure is hydrostatically distributed throughout the flow field.
- 7. The velocity, buoyancy and tracer concentration profiles are assumed similar Gaussian profiles given by the following equations:

u
$$(x,z) = w (z) \exp (-(x/b)^2)$$

g' $(x,z) = g' (z) \exp (-(x/\lambda b)^2)$
c $(x,z) - c (z) \exp (-(x/\lambda b)^2)$

Using the above equations to integrate the partial differential equations Fan and Brooks derived the following set of differential equations:

$$dq/dz = E$$

$$dm/dz = \frac{bq}{m} \left(\frac{1 + \lambda^2}{2}\right)^{1/2}$$

$$d\beta/dz = -q\varepsilon$$

$$dt/dz = 0$$

Where the Morton, or List and Imburger entrainment assumptions may be used in completing the first equation.

Use of the Program

The program determines the gross behavior of a buoyant jet. For this reason all input data must have compatible units. The input data is

read into the program through the card below:

READ
$$(5, DATA, END = 100)$$

The data is defined in the namelist below:

NAMELIST/DATA/Q,M,B,EPSS,HH,ALPHA,DEBUG,MORTON,TOL,ZDEBUG ALPHA is the Morton entrainment coefficient taken as 0.11 . If DEBUG is true, then additional printout will be added. This printout includes the intermediate calculations of the differential equation solver. If MORTON is set true, then Morton entrainment assumption is used; if false, then List and Imberger is used. TOL is set to a default value of 0.001 and represents the local error of integration. ZDEBUG is the elevation which DEBUG will be changed to true if it was initially set false. The integration steps are taken as one unit of whatever the common units of length are.

Method of Solution

Once the initial values are input, the program determines the initial values to start the integration process. The starting z is found from the equation:

$$z = 5.20^{2}/M$$

where Q and M are the initial flux values.

The coefficient $\left(\frac{1+\lambda^2}{2\lambda^2}\right)^{1/2}$, where λ is the turbulent Schmidt number, corrects the initial density difference for the zone of flow establishment. In this way the program assures that the correct initial buoyancy flux is used. From this point the subroutine is entered and one integration step is made. After returning from the differential equation solver a check is made that the local error is not too large. Then the program returns, with the newly calculated values, to the beginning of

the subroutine where the process begins again. This will continue until the water surface is reached or the momentum flux goes to zero, whichever happens first.

-- PROGRAM BJET3L --

```
PROGRAM BJET3L(OUTPUT, TAPE5, TAPE6 = OUTPUT)
2
    C....TWO DIMENSIONAL VERTICALLY DISCHARGED BUOYANT JET, INPUT TOP.....
3
    C
         HAT SLOT FLUXES Q.M.B; 3 STRATIFICATION PARAMETERS EPS = *G/RHD*DRHD/
4
    C
         DZ: 3 DEPTHS H. HH(1) IS HEIGHT = RDM SOURCE TO FIRST INTERFACE,
5
    C
         HH(2) IS HEIGHT TO SECOND, HH(3) IS HEIGHT TO WATER
    C
6
         SURFACE: MORTON ENTRAINMENT COEFFICIENT ALPHAM: SET DEBUG .TRUE.
    C
7
         FOR ADDITIONAL PRINTOUT; SET MORTON .TRUE. FOR MORTON ENTRAINMENT.
8
    C
         IF .FALSE. LIST AND IMBERGER TYPE USED. PROGRAM COMPUTES LOCAL
9
    C
         FLUXES (Q.M.B) AND MINIMUM DILUTION SM. FROM END OF ZFE TO EITHER
    Ċ,
10
         HEIGHT WHERE H BECOMES NEGATIVE OR WATER SURFACE. TOL CONTROLS
    C
         LOCAL ERROR. SET INITIALLY 0.001. ZDEBUG IS ELEVATION AT WHICH
11
         DEBUG PRINT OUT SWITCHES ON IF DEBUG=.FALSE. ON INPUT.
12
13
         REAL M
14
         LOGICAL DEBUG, MORTON
15
         EXTERNAL DERIV
16
         DIMENSION Y(3), YDOT(3), W(3.9), C(24), EPSS(3), HH(3)
17
         COMMON BLOCK 1/EPS, ALPHAM, MORTON, H. DEBUG
18
         NAMELIST/DATA/O.M.B.EPSS.HH, ALPHAM, DEBUG, MORTON, TOL, ZDEBUG
19
20
    C....READ AND WRITE INPUT AND HEADINGS; FORMATS....
21
         READ (5.DATA.END = 100)
22
         IF(MORTON) GO TO 3
23
         WRITE(6.200) Q.M.B.EPSS.HH
24
    200
         FORMAT('I VERTICALLY DISCHARGED BUOYANT SLOT JET WITH TOP HAT
25
         +SLOT FLUXES:'/'
                            O = .F10.5. M = .F10.5. B = .F10.5
         + ENTRAINMENT IS MODELED WITH THE LIST AND IMBERGER RELATIONSHIP
26
27
               THE AMBIENT FLUID HAS: EPS = '.3FB.5/' H = '.3F8.2)
28
         GO TO 4
29
         WRITE (6,201) Q.M.B.ALPHAM.EPSS.HH
30
                      VERTICALLY DISCHARGED BUOYANT SLOT JET WITH TOP HAT
         FORMAT('I
31
                                          M = `.F10.5.`
         +SLOT FLUXES:'/'
                            Q = `.F10.5.`
                                                        B = .F10.5/
32
             ENTRAINMENT IS MODELLED WITH MORTONS RELATION .ALPHAM = '.F6.3
33
               THE AMBIENT FLUID HAS: EPS = '.3F8.5/'
                                                        H = 1.3F8.2
34
         FORMAT(1H-.12X.'2'.12X.'Q'.8X.'M'.11X.'B'.11K.'SM'.3X.
    202
         +'IND'.3X.'1ER'//5X,5F12.5,216)
35
         FORMAT(* '.5X.5F12.5.2I6)
36
    203
37
         FORMAT(' '.'DEBUG 11'/5X, 'Z,Y1,2,3,Z2,EPS, +,IND,1ER; ',7F12,5,
38
         +5X.216)
39
    209
        FORMAT (' '.'DEBUG 13'/5X, 'Z.Y1,2,3,Z2,EPS.H,IND,IER:',7F12,5.
40
41
         COEFF = SQRT(1.35 + 1.35/(1. + 1.35*1.35))
    C
42
43
44
    C....INITIAL VALUES USED TO BEGIN INTEGRATION.....
45
         Z = 5.2*O**2/M
46
        Y(1) = Q*1.414
47
        Y(2) = M
48
        Y(3) = B
49
        SM = COEFF*Y(1)/Q
50
         WRITE(6.202) Z.Y(1).Y(2).Y(3).SM
51
        DO 2 1 = 1.9
```

PROGRAM BJET3L (CONTINUED)

```
52 2
          C(1) = 0.0
53
          C(9) = 1.
54
          DELTA = 1.
55
          EPS = EPSS(1)
56
          H = HH(1)
57
          I = 1
58
    C
59
    C....BEGIN INTEGRATION LOOP.....
60
         Z2=Z+1
         IF(Z2.GT. H) Z2=H
61
          IND=2
62
63
          IF (Z .GT. ZDEBUG) DEBUG=.TRUE.
64
    11
         IF (DEBUG) WRITE (5,207) Z.Y(1).Y(2).Y(3),Z2.EPS.H,IND.EIR ·
65
         CALL DVERK (3.DERIV.Z,Y,Z2.1.E-3.IND.C.3.W.IER)
66
         CALL DERIV(3,Z,Y,YDOT)
67
         IF(YDOT(2) .LT. 0.0) GO TO 80
68
         GO TO 13
    80
         DELTA = ABS(Y(2)/YDOT(2))/Z
69
70
         IF(DELTA .LT. 0.005) GO TO 15
71
    13
         IF(DEBUG) WRITE(6.209) Z.Y(1).Y(2).Y(3).Z2.EPS.H.IND.1ER
         IF(DEBUG) PRINT*,C.W
    14
72
73
         IF(IND .EO. 5 .OR. IND .EO. 6) GO TO 6
74
         SM = COEFF*Y(1)/Q
75
         WRITE(6.203) Z.Y(1),Y(2),Y(3),SM.IND.IER
76
         IF(IND .LT. O .OR. IER .GT. O) GO TO 20
         IF(DELTA .LT. .005) GO TO 30
77
78
         IF(F ZEG. H) GO TO 39
79
         GO TO 30
80
    20
         WRITE (6,204) IND. IER
    264 FORMAT (1HD.' PROBLEMS WITH INTEGRATION. IND='.15' IER='.
81
82
          +15)
83
         GO TO 99
84
    30
         .RITE (6,205)
85
    205 FORMAT (IHD,' REACHED TERMAL HEIGHT')
86
         GO TO 99
87
    39
         1 = 1 + 1
88
         IF(I .EQ .4) GO TO 40
89
         EPS = EPSS(I)
90
         H = HH(I)
91
         GO TO 10
92
    40
         WRITE (6.206)
93
    206 FORMAT (IHD.' REACHED WATERSURFACE')
94
    99
         PRINT*,C,W
95
         GO TO I
96
    100 STOP
97
         END
```

SUBROUTINE

```
C
C
2
3
    C
4
         SUBROUTINE DERIV (NDER, Z, Y, YDOT)
5
         LOGICAL MORTON. DEBUG
         DIMENSION Y(3), YDOT(3)
7
         COMMON/BLOCK1/EPS.ALPHAM.MORTON,H.DEBUG
8
         PI = 3,1416
9
         IF(MORTON) GO TO 5
10
    C....LIST AND IMBURGER ENTRAINMENT.....
11
12
         IF (Y(2) .LE. 0.8) GO TO 55
13
         RO = Y(3)*Y(1)**3/Y(2)**3
14
         IF (RO .LT. 0.0) RO=0.0
15
         GO TO 56
16
    55
         RO = 0.0
17
    56
         E = 2.828*Y(2)/Y(1)*(0.855+0.87*RO)
18
         GO TO 6
19
20
   C....MORTOM ENTRAINMENT RELATONSHIP.....
21
    5
         E = 2.828*ALPHAM*Y(2)/Y(1)
22
         CONTINUE
    6
23
         YDOT(1) = E
         YDOT(2) = SQRT(1.+1.35*1.35)/2.)*Y(1)*Y(3)/Y(2)
24
25
         YDOT(3) = -Y(1)*EPS
26
         IF(DEBUG) WRITE(6.210) Z,Y(1),Y(2),Y(3),YDOT(2),YDOT(3),EPS,H
   210 FORMAT(' '.'DEBUGDERIVI',5X, 'Z,Y1,2,3,EPS.H:'/5X.
27
28
         +8F12.5)
29
         RETURN
30
         END
```



BIBLIOGRAPHY

- Buhler, J. (1974), "Model Studies of Multiport Outfalls in Unstratified, Stagnant or Flowing Receiving Water," Ph.D. Thesis, University of California at Berkeley.
- Fan, L. N. and Brooks, N. H. (1969), "Numerical Solutions of Turbulent Buoyant Jet Problems," <u>Tech. Rep. KH-R-18</u>, W. M. Keck Laboratory of Hydraulics and Water Resources, California Institute of Technology, Pasadena, California.
- Feuerstein, D. L. and Selleck, R. E. (1963), "Fluorescent Tracers for Dispersion Measurements," <u>J. San Eng. Dis.</u>, ASCE, Vol. 89, SA4, pp. 1-21.
- Fisher, H. B., et al. (1979), <u>Mixing in Inland and Coastal Waters</u>. New York, Academic Press.
- Hart, W. W. (1961), "Jet Discharge into a Fluid with a Density Gradient," J. Hyd. Div., Proc. ASCE 87, HY6, November.
- Jirka, G., and Harleman, D. R. F. (1973), "The Mechanics of Submerged Multiport Diffusers for Buoyant Discharges in Shallow Water," Ralph M. Parsons Laboratory for Water Resources and Hydrodynamics, Massachusetts Institute of Technology, Report No. 169.
- Koh, R. C. Y. (1976), "Buoyancy-Driven Gravitational Spreading," Proc. 15th Int. Conferences Costal Engineering, July 11-17, Honolulu, Hawaii, Vol. 4, pp. 2956-2975.
- Roberts, Philip J. W. (1977), "Disperson of Buoyant Wastewater Discharged from Outfall Diffusers of Finite Length," W. M. Keck Laboratory of Hydraulics and Water Resources, Report No. KH-R-35, California Institute of Technology, Pasadena, California.
- Roberts, Philip J. W. (1981), "Jet Entrainment in Pumped-Storage Reservoirs," Technical Report #ME-81-3, prepared by Georgia Institute of Technology, Atlanta, Georgia, for the U.S. Army Engineer Waterways Experiment Station, CE, Vicksburg, Mississippi.
- Schatzmann, M. (1977), "Buoyant Jets in Natural Flows: Development of Mathematical Model: Translation of a German Report," Thesis, Department of Energy, University of Karlsrue, West Germany.
- Sotil, C. A. (1971), "Computer Program for Slot Buoyant Jets into Stratified Ambient Environments," W. M. Keck Laboratory of Hydraulics and Water Resources, California Institute of Technology, Pasadena, California.

- Wallace, R. B. (1981), "Two-Dimensional Buoyant Jets in a Stratified or Crossflowing Ambient Fluid," Dissertation presented to the University of Michigan, Ann Arbor, Michigan, in partial fulfillment of the requirements for the degree of Doctor of Philosophy.
- Wallace, R. B. and Wright, S. J. (1980), "Buoyant Jet Behavior Neat the Maximum Rise," <u>J. Hyd. Div., ASCE</u>, Vol. 105, No. HY11, November.
- Willard, H. H., et al. (1981), <u>Instrumental Methods of Analysis</u>. Belmont, California, Wadsworth Publishing Company.
- Wright, S. J. and Wallace, R. B. (1979), "Two-Dimensional Buoyant Jets in a Stratified Fluid," <u>J. Hyd. Div., ASCE</u>, Vol. 105, No. HY11, November.

